Departement für Kleintiere, Klinik für Kleintierchirurgie

der Vetsuisse-Fakultät, Universität Zürich

Direktor: Prof. Dr. Pierre Montavon

Arbeit unter Leitung von Prof. Dr. Keita Ito

Hydroxyapatite particles maintain peri-implant bone mantel in osteoporotic bone

Inaugural-Dissertation

zur Erlangung der Doktorwürde der

Vetsuisse-Fakultät Universität Zürich

vorgelegt von

Michelle Gertrud Baucke

Tierärztin

aus Werneck, Deutschland

genehmigt auf Auftrag von

Prof. Dr. Pierre Montavon, Referent

Prof. Dr. Keita Ito, Korreferent

Zürich 2008

Department für Kleintiere

Klinik für Kleintierchirurgie

Direktor: Prof. Dr. P. Montavon

AO Forschungsinstitut

Gruppe der Mechano Biology

Gruppenleiter: Prof. Dr. Keita Ito

HYDROXYAPATITE PARTICLES MAINTAIN PERI-IMPLANT BONE MANTEL IN OSTEOPOROTIC BONE

vorgelegt von

Michelle Gertrud Baucke

TABLE OF CONTENTS

SUMMARY

In osteoporotic bone, bone resorption exceeds bone formation resulting in decreased bone volume and bone contact in the peri-implant region. Subsequently, implant loosening may occur. Current approaches to reduce the effect of remodelling on secondary implant stability focus mainly on pharmaceutical methods. In this study we investigated a surgical alternative based on particles of a non-resorbable, osteoconductive hydroxyapatite ceramic (HA) clinically used as bone filler. We hypothesized that the presence of such particles could help maintaining a denser and more functional peri-implant bone structure and shift remodelling events. Threaded titanium screws were implanted into the proximal tibial metaphysis of four months old Wistar rats, four weeks after ovariectomy. In the right tibia, the drill hole was filled with HA particles before screw insertion, while the left tibia served as a control without HA particles. Rats were sacrificed at five different time points in the following eight weeks. Histological analysis demonstrated that during the remodelling phase the amount of newly formed bone was significantly higher on the HA over the control side. These results indicate that HA particles are able to induce and maintain for a longer time a denser peri-implant bone mantel in osteoporotic bone, which may have significant implications in implant anchorage and in prevention of implant migration and cut-outs.

INTRODUCTION

Osteoporosis is a systemic skeletal disease characterized by low bone mass and micro-architectural deterioration of bone tissue with a consequent increase of bone fragility and susceptibility to fractures. Osteoporosis affects about 75 million people in Europe, Unites States and Japan [1], mostly aged 50 and older. Of the 10 million Americans estimated to have already osteoporosis, 80 % are women [2]. The annual incidence of osteoporotic fractures exceeds 1.5 million in the Unites States [3]. In Switzerland, the total estimated cost due to osteoporosis and related fractures was 357 million CHF and represented the leading causes of direct medical costs [4]. Most of them are from low-energy falls, including especially proximal femur fractures, spine and distal radius fractures, but any bone can be affected [2,3,4]. Fractures resulting from osteoporosis generally involve the metaphyseal regions of the bones. These regions are affected earlier and even more profoundly during the development of osteoporosis. They consist mostly of cancellous bone, which offers a greater surface area for bone turnover compared with the compact cortical bone of the diaphysis. Therefore, when the bone turnover mechanisms are no longer balanced as in the case of osteoporosis, and bone resorption exceeds bone formation, the loading capability of cancellous bone is more rapidly compromised [2,5]. Osteoporotic fractures cost the United States health care system approximately $17 billion annually, with an increase of annual cost projected to approach $50 billion by the year 2040 [6].

In osteoporotic fracture repair, failure rates of up to 50% have been reported, mostly due to an implant pull-out or cut-through [5,7]. One of the reasons for this is the altered remodelling condition in osteoporotic bone, whereby bone resorption exceeds bone formation [8]. Consequently, due to the remodelling of woven bone, consisting

of a disorganized structure, into the highly organized structure of lamellar bone, bone volume, bone mineral density and bone contact decrease in the peri-implant region [9]. As a result, the supporting ability of the implant is reduced and loosening of the implant may occur.

There are many different approaches to improve implant stability in the osteoporotic patient. Some studies are based on pharmaceutical methods with the use of estrogen, calcitonin, parathyroid hormone or biphosphonates administration [10,11,12,13]. Other groups are focusing on the features of implant surfaces (e.g. hydroxyapatite coated screws) [14,15], or combine this with the treatment of prostaglandin receptor agonists [16]. Injectable bone substitutes are also of interest for this purpose [17].

Endobon® (Biomet Orthopaedics GmbH, Kerzers, Switzerland) is a commercially available non-resorbable hydroxyapatite ceramic (HA) derived from bovine cancellous bone. The basic and highly attractive profile of this material is due to its lack of local or systemic toxicity and inflammatory body response and its apparent ability to become directly bonded to bone. A series of animal and clinical trials verified its good biocompatibility, osteoconductive and even osteoinductive character [18,19,20]. It is clinically used since 1991 as bone filling material for the management of bone defects especially at tibia plateau fractures, calcaneal and distal radius fractures as well as bone cysts [21,22].

The purpose of this study was to determine whether HA particles inserted around a screw could induce an increase in peri-implant bone mass and bone-to-implant contact in an osteoporotic rat model. Previous studies with HA-coated implants demonstrated higher bone-to-implant contact which led to a better implant stability compared to uncoated implants [15,23]. Therefore, we hypothesized that the

combination of HA's osteoinductive and osteoconductive properties together with the larger available surface offered with loose particles compared to an implant coating would induce more bone formation, both in direct contact with the implant surface as well as between the bricks of HA. Another study showed that during the remodeling phase bone volume and bone-to-implant contact were reduced in osteoporotic bone compared to sham-operated animals [14]. Thus, we hypothesized that the incorporation of non-resorbable HA particles within the newly formed bone might act as a barrier to osteoclastic activity reducing bone resorption during the remodelling phase.

If our hypothesis were proven true, the presence of HA particles could offer a double positive effect on implant anchorage: 1) directly augment peri-implant bone material delivering a stronger frame for screw stability and 2) preserve more bone for a longer time in the peri-implant region by affecting remodeling. If screw stability in osteoporotic bone were improved and prolonged by the presence of HA particles, a fracture would have more time to heal before bone loosening processes of osteoporotic disease could lead to implant failure.

This thesis research work was part of a larger study. Surgery and pQCT were done by Dr. Melanie Pucher. The histological analysis was done by the author.

MATERIAL AND METHODS

Rat Model

The procedure for animal care, experimental protocol and euthanasia in this study was approved by the Animal Experimentation Commission of the Veterinary Office of the Canton of Grison, Switzerland and followed the guidelines of the Swiss Federal Veterinary Office for the use and care of laboratory animals. Twelve week old female Wistar rats were purchased from RCC (Resulting & Consulting Company AG, Basel, Switzerland). They were acclimatized for four weeks, housed in Makro Type 4 cages in groups of four and fed with standard rodent chow (Provimi, Provimi Kliba AG, Kaiseraugust, Switzerland) and water ad libitum. The rats were divided randomly into five groups of bilateral ovariectomized (OVX) animals (n=40), representing the different time-points of euthanasia after implantation and one group (n=8) of sham animals. Four weeks were then allowed to pass prior to implantation to induce significant bone loss in the OVX animals. The osteoporotic state of each animal was verified with *in vivo* bone mineral density (BMD) measurements of the distal femoral metaphyses at the time of ovariectomy as well as four weeks later using a peripheral quantitative computed tomography (pQCT) system (XtremeCT®, SCANCO Medical, Brüttisellen, Switzerland). Sham animals were then euthanized and OVX animals received titanium implants into the left and right proximal metaphysis of the tibia. Prior to screw implantation in the right tibia, the drill-hole was filled with 6mg HA particles. Animals were sacrificed either at 1 hour, 2, 4, 6 or 8 weeks post implantation by CO_2 inhalation (Fig. 1). The proximal tibiae were explanted, freed from soft tissue and fixed in methanol for histological preparation.

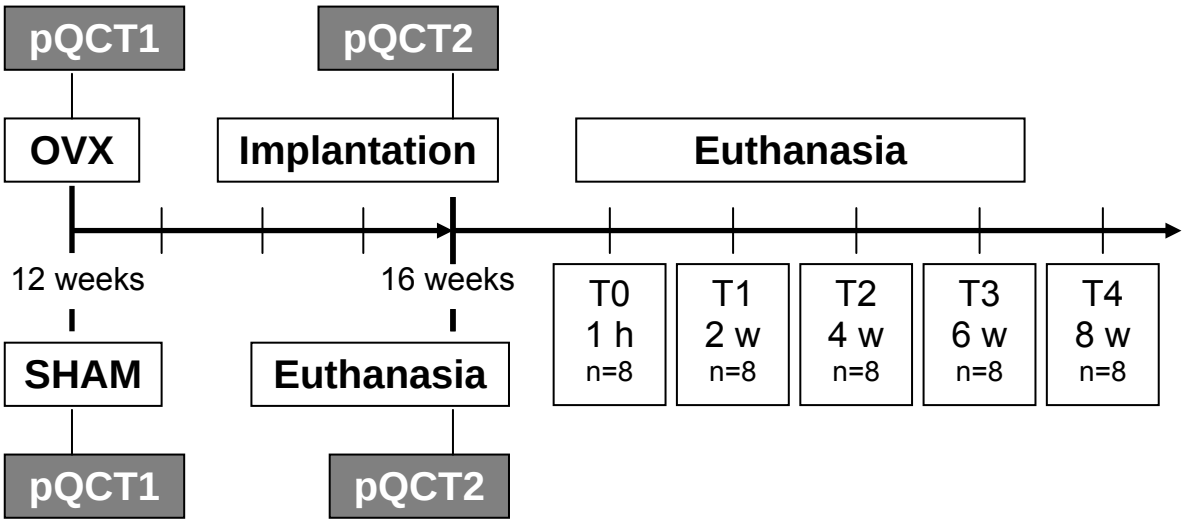

Fig. 1: Experimental design. Ovariectomy (OVX) or sham operation (SHAM) at 12 weeks, screw implantation four weeks later, and sacrifice at five different time points.

Implantation

Under aseptic conditions, a bilateral anteromedial approach was made to gain access to the proximal medial aspect of the tibia metaphysis. A hole with a diameter of 1.1 mm was drilled through one of the cortices using a custom made surgical aiming device (AO Development Institute, Davos, Switzerland) for reproducible screw positioning (Fig. 2). Profuse saline irrigation was applied to avoid bone thermal necrosis (Fig. 3). A self-tapping titanium screw (Ø 1.7 x 5 mm) was inserted bilaterally (Synthes®, Oberdorf, Switzerland). A 1 mm thick polyethylene washer was placed under the screw head, and acted as a place-holder for subsequent pull-out tests to measure ultimate force and stiffness of the anchorage (Fig. 2). The drill-hole in the right tibia was filled with 6 mg HA ceramic particles prior to screw insertion, whereas the left tibia served as control and the screw was implanted without HA particles (Fig. 2). Fascial and cutaneous tissues were closed in two separate layers.

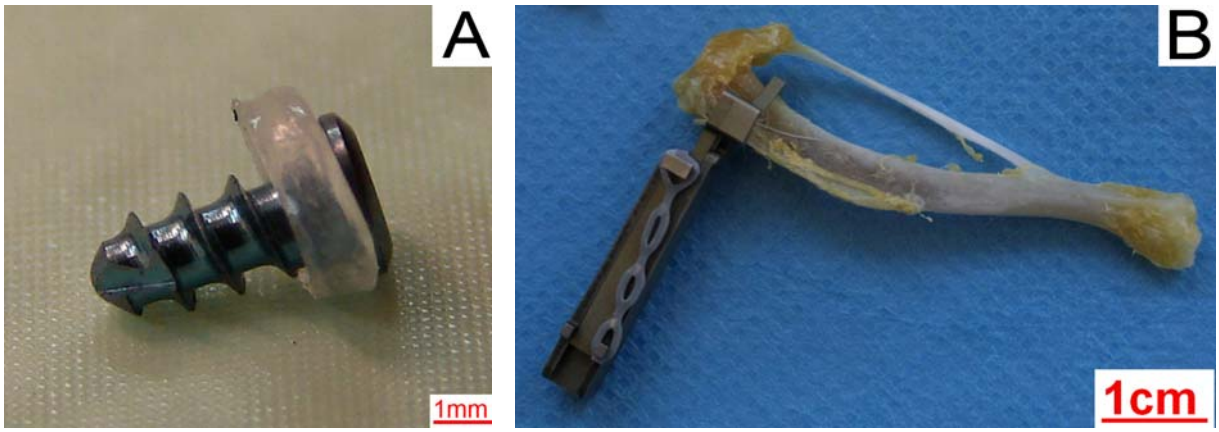

Fig. 2: Threaded titanium implant with polyethylene washer (A). Custom made jig for accurate and reproducible screw insertion, placed at the proximal tibia of the rat (B).

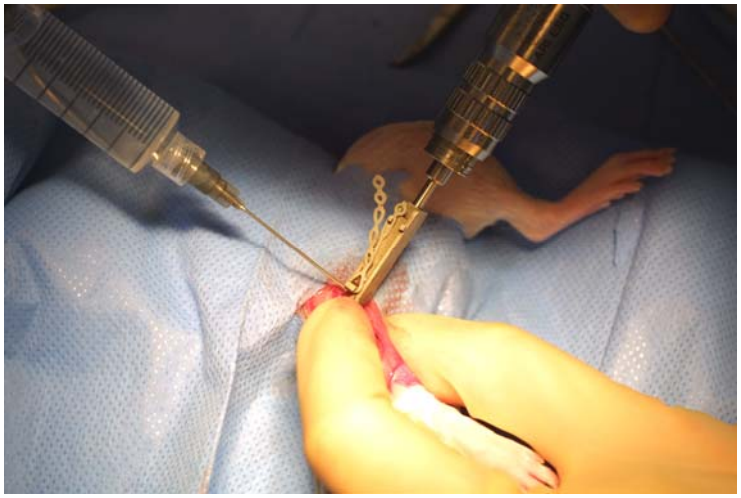

Fig. 3: Surgical procedure: screw insertion under saline irrigation in the proximal right tibia using a custom made jig.

HA particles

Endobon® (Biomet Orthopaedics GmbH, Kerzers, Switzerland) is a non-resorbable hydroxyapatite ceramic (HA) derived from bovine cancellous bone. These natural particles with a size of approximately 1.5 mm are modified through physicochemical treatment such as pyrolysis of over 900 °C followed by a vitrification process of 1200 °C to remove potential pathogens [24].

The purchased particles were ground and separated using two sieves (Fritsch GmbH, IDAR-Oberstein, Germany) with a mesh width of 63 and 100 μm. Particles remaining between those sieves were gas-sterilized and 6 mg samples were prepared.

Fig. 4: Endobon granules (Biomet, Switzerland) after grinding and sieving procedures.

pQCT

pQCT was performed using an XtremeCT® (Scanco Medical, Brüttisellen, Switzerland). This scanning system consists of a two-dimensional detector array with 3072x255 elements in combination with a microfocus X-Ray-tube having a spot size of 70 µm, enabling simultaneous acquisition of a stack of parallel CT slices. The rat was positioned on an in-house custom made holder made of plexiglas, which allowed consistent and precise positioning of the rat leg. The longitudinal axis of the left leg was aligned perpendicular to the scanner beam. Fifty-three cross-sectional slices (corresponding to a length of 2 mm) were collected at the distal femoral metaphysis with an isotropic voxel resolution of 41 µm and a pixel matrix of 3072x3072, using an effective energy of 60 keV and a current intensity of 900 µA. The total scanning time was 10 minutes. The resulting gray-scale images were then processed using a

Gaussian low-pass filter (sigma=0.7, support=1) to remove noise, and apparent bone mineral density (BMD) was calculated for the cancellous bone region. For accurate matching of the 2-mm-long region of interest (ROI), an anatomical reference point was defined. The most proximal aspect of the distal femoral growth plate was chosen for this landmark.

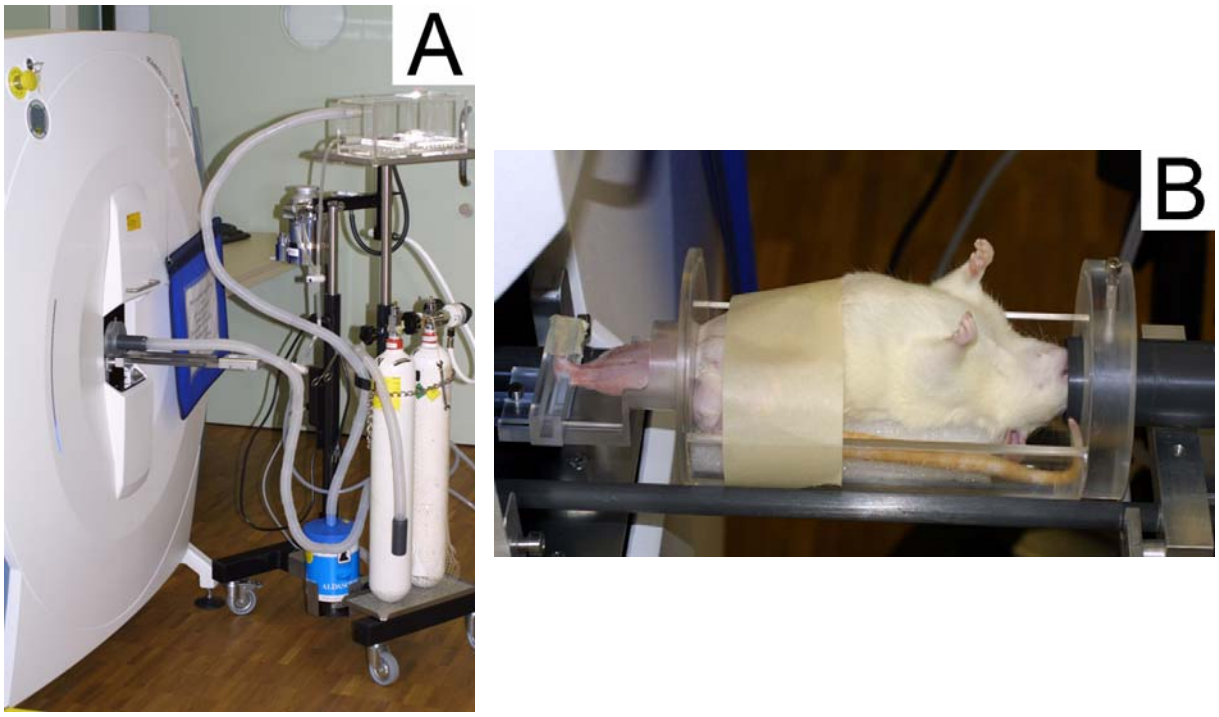

Fig. 5: XtremeCT and mobile anaesthesia device for in vivo pQCT measurements (A). Plastic holder to scan the distal femur in a consistent and repeatable way while keeping the rat anaesthetized (B).

Histology

Processing

Tibiae (n=8 for each time point and group) were fixed in methanol, embedded undecalcified in polymethylmethacrylat (PMMA) and serially sectioned to a thickness of 250-300 μm using a circular saw (Leitz SP 1600 Saw microtome®, Leica AG, Glattbrugg, Switzerland) (Fig. 6). Two mid-sagittal sections of each screw were ground and polished to a final thickness of approximately 120-160 μm (Exakt Micro Cutting-Grinding System®, Exakt Apparatebau, Norderstedt, Germany) (Fig. 7).

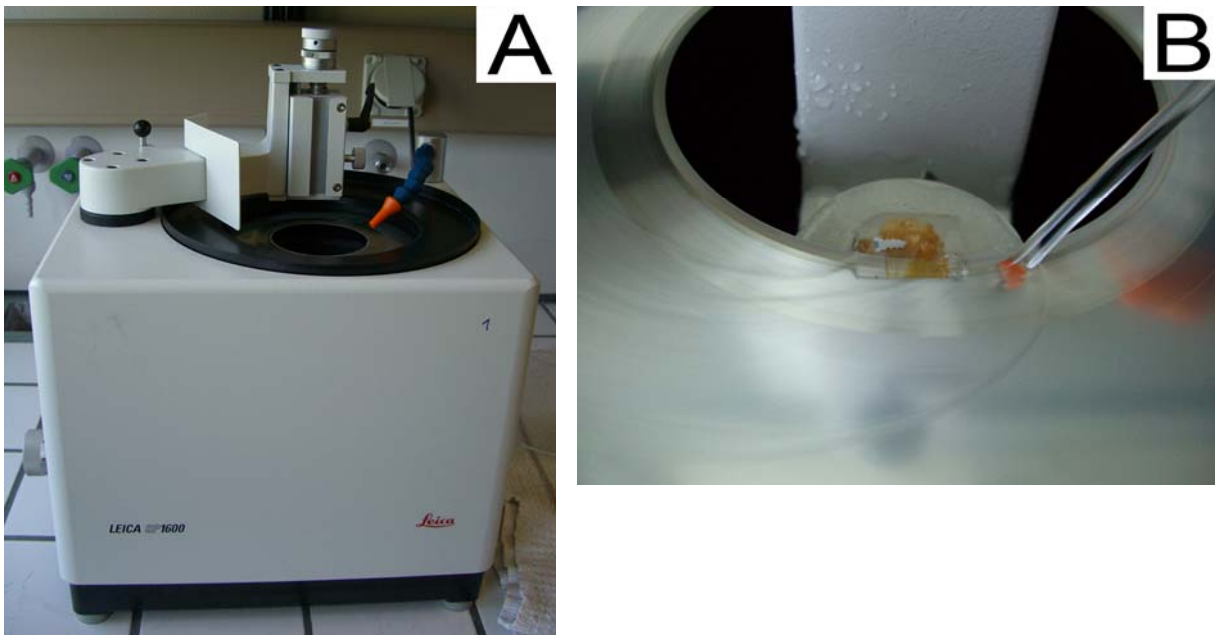

Fig. 6: Circular saw (Leica, Switzerland) (A). Sectioning procedure of one sample (B).

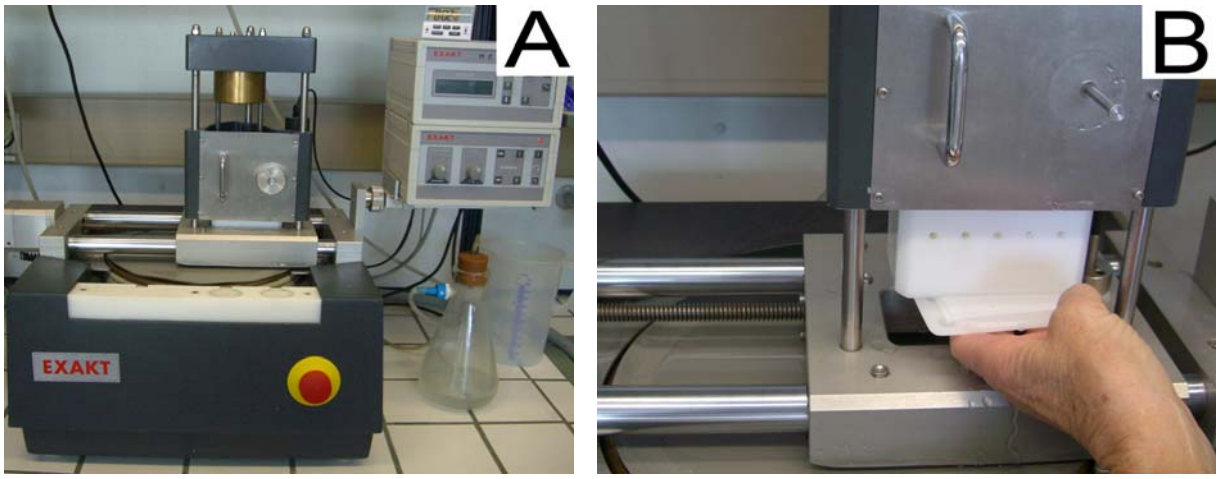

Fig. 7: Sample ground under water irrigation (Exakt Apparatebau, Germany) (A). Sample was held on the grinding machine by vacuum (B).

Each section was stained for microscopic observation. The surface was etched with 1% formic acid (Fluka, Buchs, Switzerland) for 30 seconds and rinsed with deionized water. For quantitative morphological analysis sections were stained with 1% Toluidine blue (Fluka) for 17 minutes and blot dried after washing in deionized water. For qualitative evaluation and comparison of cell activity, sections were blot dried, and stained with 15 % Giemsa (Fluka) for 45 minutes under 57ºC heat. After controlling the intensity of Giemsa under light microscopy, the samples were stained with 1% Eosin Yellowish (Fluka) for three minutes. Finally, the sections were rinsed in increasing ethanol concentrations.

Analysis

Combining transmitted bright field and reflected dark field microscopy (Axiotech® Imaging microscope, Carl Zeiss AG, Feldbach, Switzerland), 12-14 images for each section were collected at x100 magnification using AxioVision software (Carl Zeiss AG, Feldbach, Switzerland). Those images were then aligned and stitched together using Adobe® Photoshop (Adobe Systems GmbH; Zurich, Switzerland) (Fig. 8).

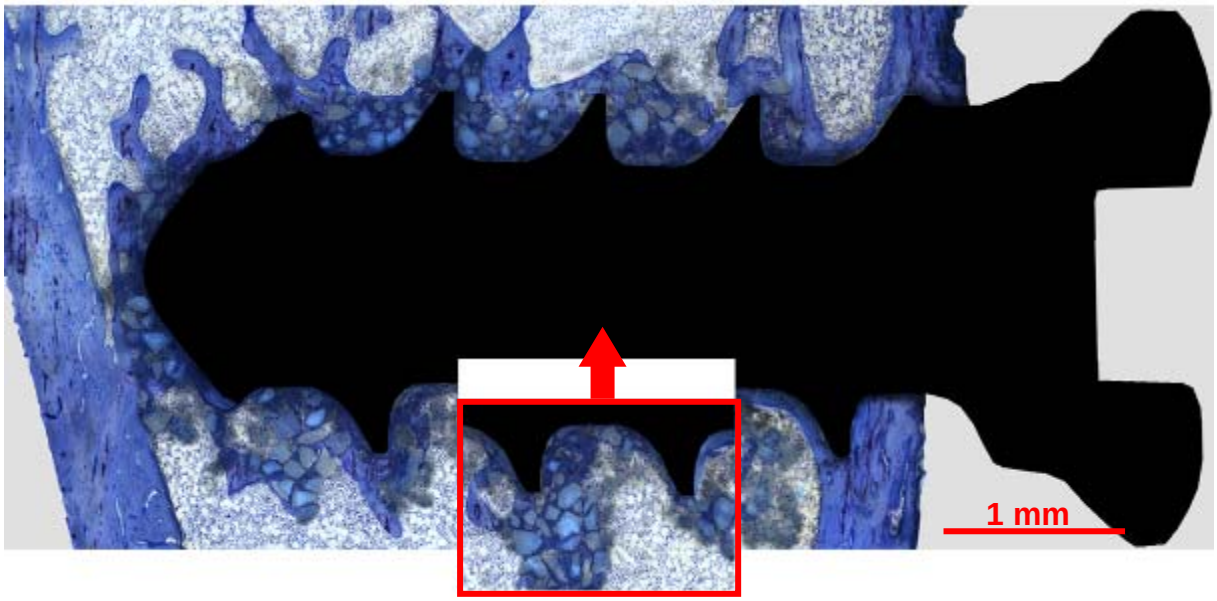

Fig. 8: Twelve images of one section collected at x100 magnification and stitched together. One displaced image to highlight the size of a stitched image (toluidine blue, original magnification x100).

A 500 µm thick peri-implant ROI was measured from the inner diameter of the screw. Two sub-regions were defined to separate the threaded region, where the full thread began by screening all the samples, in a proximal and distal part (Fig. 9). The exact same threaded region with a length of 1900 µm was selected for all samples. Lamellar bone, woven bone, HA particles and mineralized epiphyseal cartilage were differentiated and manually contoured within the ROI (Fig. 10).

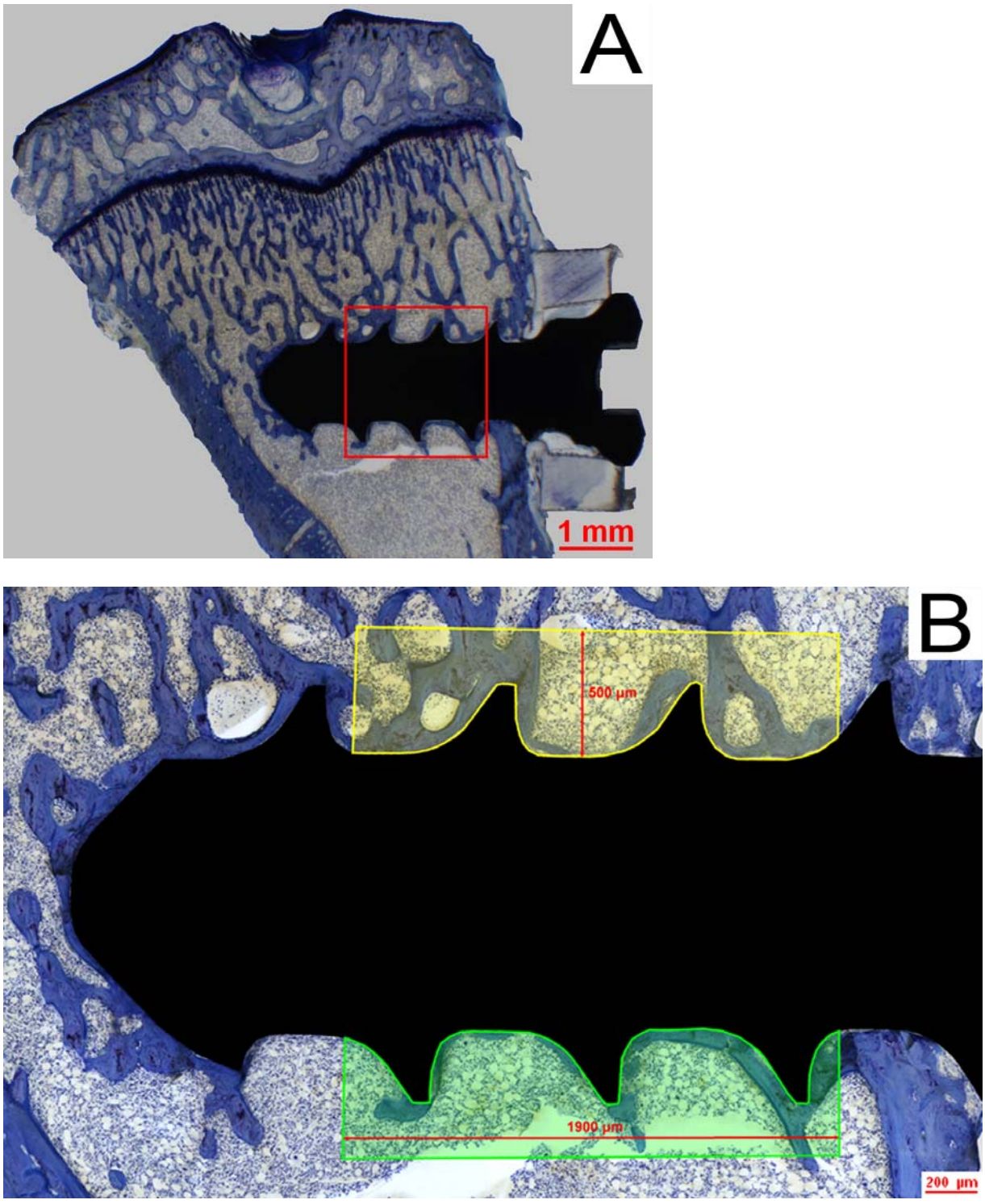

Fig. 9: Overview of the position of the screw with its caption in the proximal tibia with marked threaded region of interest (A). Two 500 µm thick peri-implant sub-regions with a length of 1900 µm (B): proximal region (yellow), distal region (green) (toluidine blue, original magnification x100).

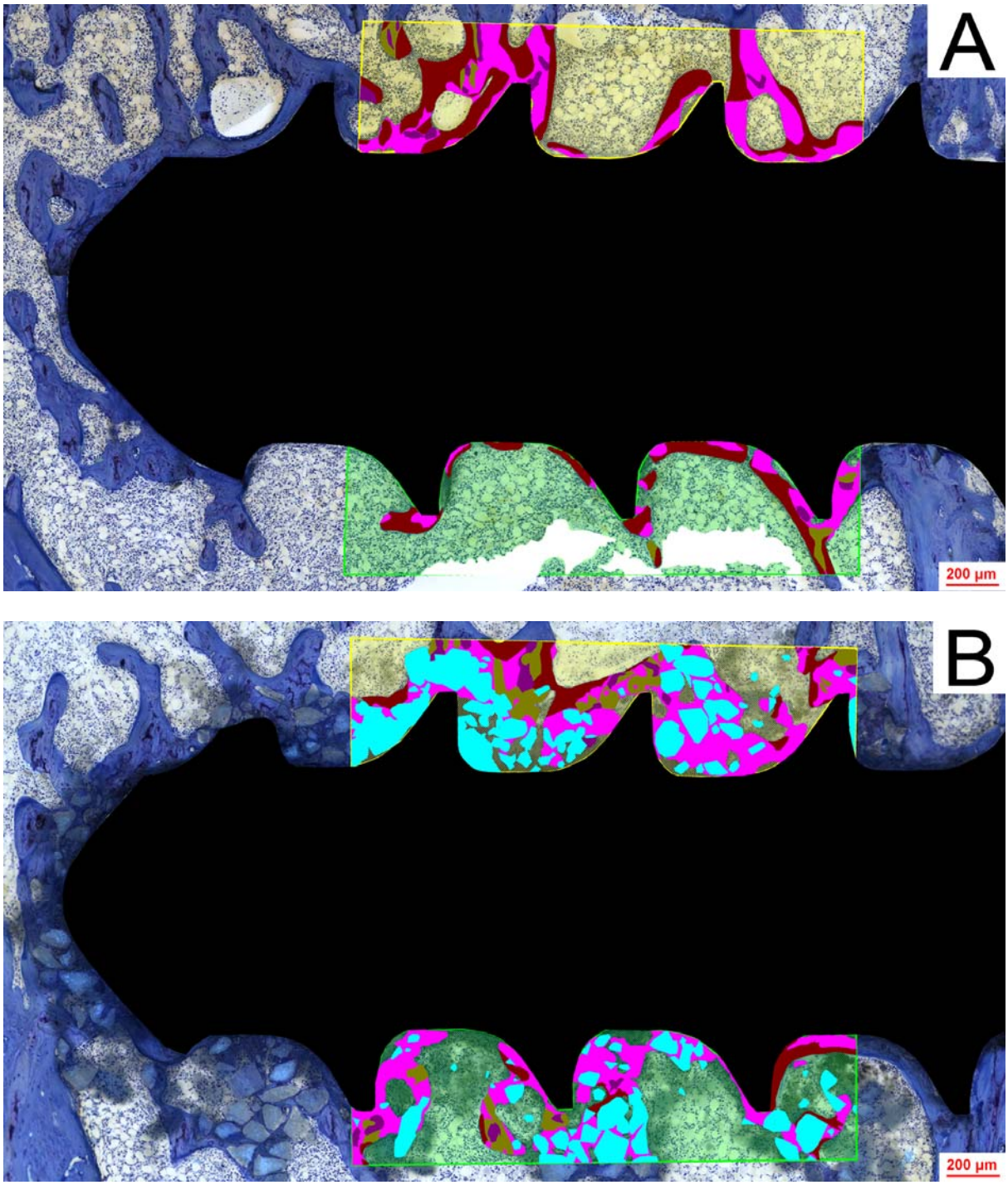

Fig. 10: A: control side; B: HA side: Differentiation and manual contouring of new woven bone (fuchsia), new lamellar bone (maroon), mineralized epiphyseal cartilage (purple), primary remodelled epiphyseal bone (olive) and HA particles (aqua) in the threaded region (toluidine blue, original magnification x100).

For each of the sub-regions the amount of bone material representing the percent surface occupied by each bone type and HA particles were quantified. The contact rate, i.e. the percent of screw surface covered by bone types and HA particles was also quantified at all time-points. Following parameters were assessed using a custom-made macro (KS 400 3.0, Carl Zeiss AG, Feldbach, Switzerland) (Table 1).

measured parameters (pixel)	definition
Area of sub-regions	Total area of each of the two sub-regions.
Area of bone types and HA	Total area of either woven bone, lamellar bone, primary remodelled lamellar bone, epiphyseal cartilage or HA particles within each sub-region.
Implant surface	Total length of implant's outline in each sub-region.
Contact length of bone types and HA	Total length of implant's perimeter in contact with a specific type of bone or HA.
calculated parameters (%)	
Percent area	Area of a specific bone type or HA divided by area of a sub-region.
Percent contact	Contact length of a specific bone type or HA divided by implant's perimeter.

Table 1: Measured and calculated parameters assessed with the quantitative evaluation protocol.

Toluidine blue sections of the proximal tibiae were additionally examined using a transmitted bright field macrofluoroscope (MacroFluo™, Leica Microsystems, Glattbrugg, Switzerland) to estimate the longitudinal bone growth rate. The distance between screw axis and growth plate of the proximal tibia was defined as the mean between the largest and smallest distance (Fig. 11).

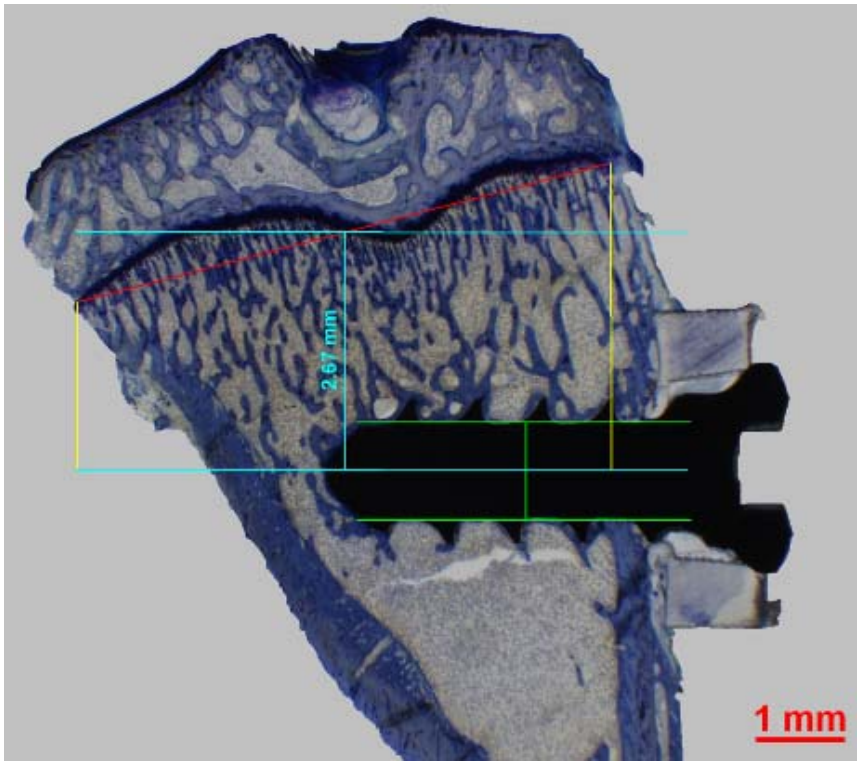

Fig. 11: Screw positioned with its caption in the proximal tibia (control side). Estimated longitudinal bone growth rate: the distance was defined as the mean (blue line) of the largest (right yellow line) and smallest (left yellow line) distance between screw axis and growth plate (green line: screw diameter) (toluidine blue, original magnification x16).

Samples stained with Giemsa/Eosin were qualitatively evaluated using the same combined transmitted bright field and reflected dark field microscopy (Axiotech® Imaging microscope, Carl Zeiss AG, Feldbach, Switzerland) as for the analysis of toluidine blue staining sections with a magnification between 25 and 500 (Fig. 12).

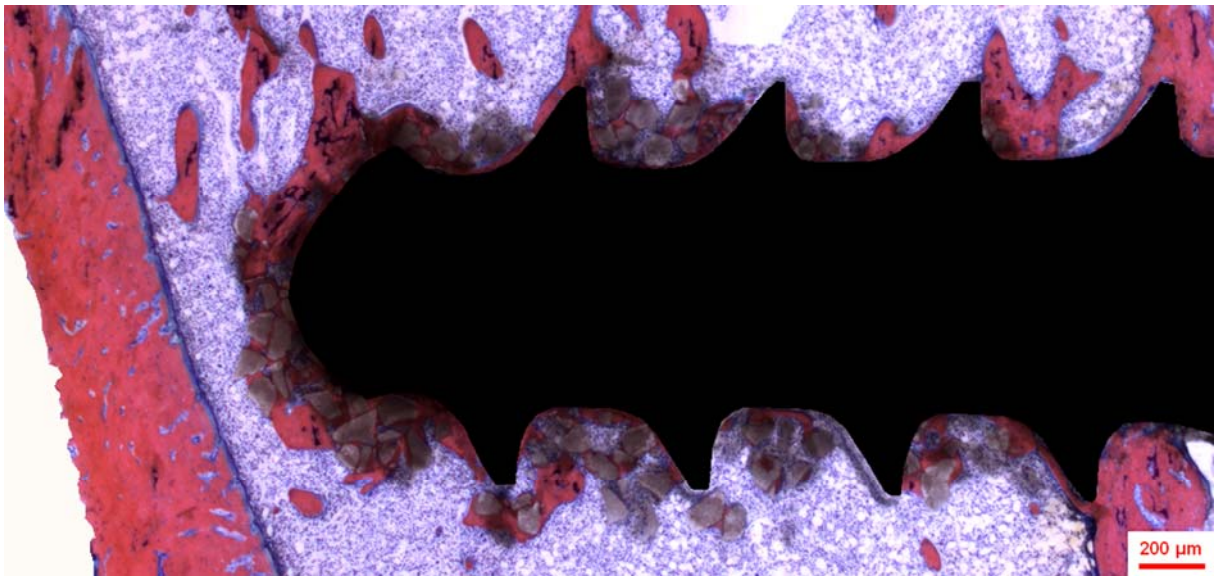

Fig. 12: Overview of the peri-implant region (Giemsa/Eosin, original magnification x25).

First, the sections were screened with respect to cellular activities, especially inflammation, fibrosis and other adverse effects, but also with regard to remodelling units due to the presence of HA ceramic. Moreover, as an additional staining, the results of the quantitative analysis could be supported and visualized, e.g. bone formation during the experimental period.

Statistical analysis

Analyses of the quantitative results were carried out using SPSS software (SPSS Science, 14.0 for Windows Chicago, IL, USA). A p-value of 0.05 was used as a threshold for statistical significance. Deviations from normal distribution were determined with Shapiro-Wilk test. To analyse the difference in peri-implant bone mantel or bone contact over time and between treatment groups an analysis of variance was performed with treatment and time as factors in a full factorial General Linear Model using a Tukey HSD post-hoc test. In the case of significant interaction between the two factors, a One-Way ANOVA with Tukey HSD post-hoc test for “time” and a paired T-test for “treatment” were performed separately.

RESULTS

pQCT

Ovariectomy in rats caused a mean decrease in apparent cancellous bone mineral density of 33.9% at the distal femoral metaphyses after four weeks compared to age-matched sham operated animal. Based on the definition of the World Health Organization, the resulting T-score of -2.8 (i.e.: OVX-group 324±56 mgHA/ccm vs. SHAM-group 491±60 mgHA/ccm) corresponds to an osteoporotic state of the bone tissue (Fig 13).

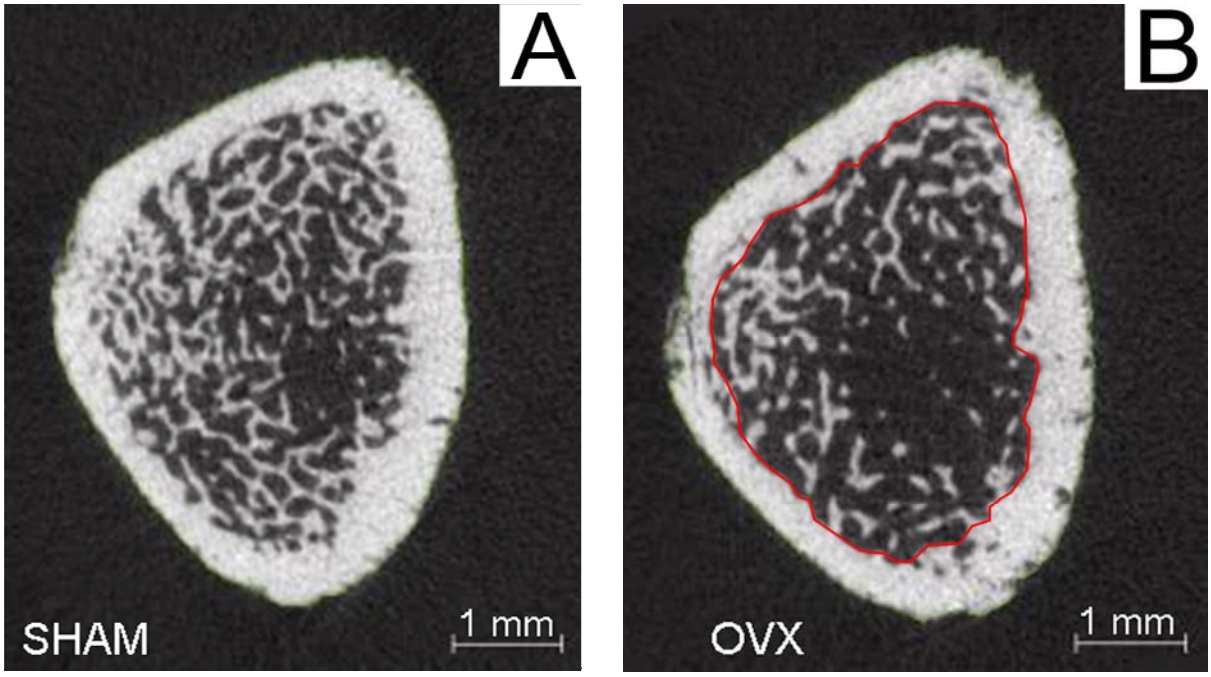

Fig. 13: Cross-section of a sham-operated (A) and an ovariectomized (B) sample. Apparent decrease of cancellous bone mineral density (within contour) in the distal femoral metaphysis (B).

Histological analysis

Data from HA and control side at all time points were normally distributed.

1. Quantitative Analysis

1.1. Bone mass and contact rate

Results from the quantitative analysis done with toluidine blue staining demonstrated that the total amount of peri-implant newly formed bone, which results from the addition of newly formed lamellar and woven bone together, was significantly higher ($p < 0.001$) in the HA side compared to the control side between six and eight weeks after screw insertion (Fig. 14).

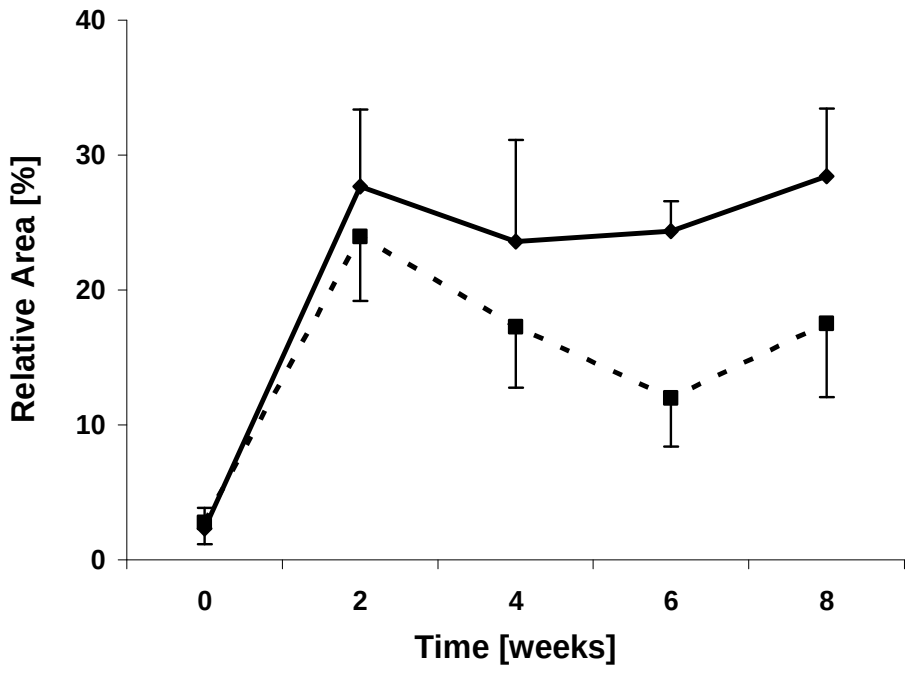

Fig. 14: Amount of newly formed bone (i.e. lamellar bone and woven bone added together) in the thread region (—: HA side, ---: control side). Error bars indicate standard deviation (SD).

Lamellar bone significantly increased with time in a similar way on both sides ($p = 0.001$). Woven bone increased abundantly and also in a similar way during the first two weeks, however, it was subsequently resorbed differently ($p = 0.001$). Woven bone area percentage remained significantly higher on the HA side compared to the control side for the remaining experimental period ($p < 0.001$) (Fig. 15).

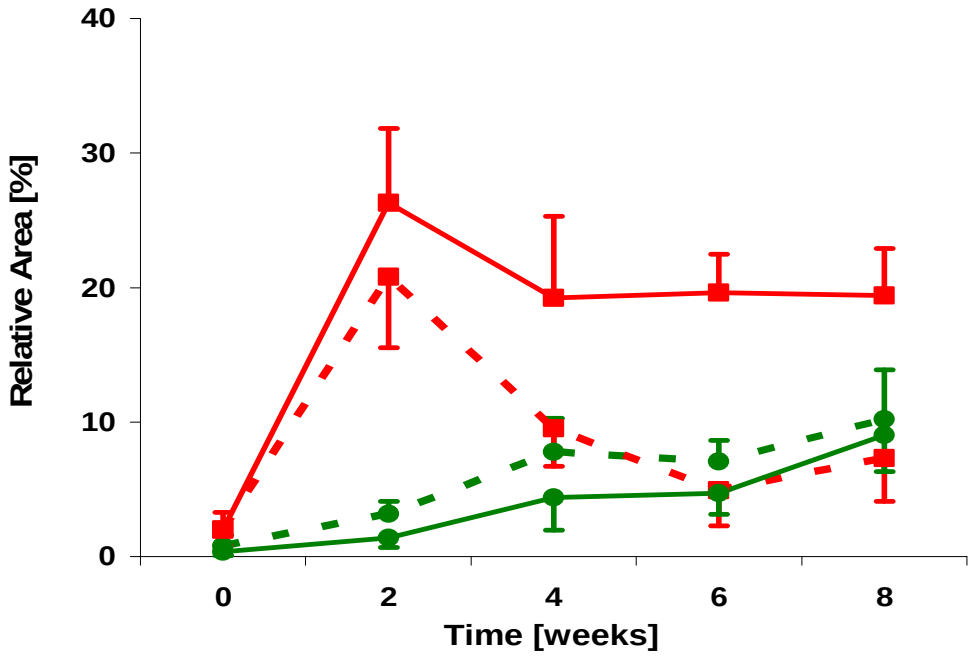

Fig. 15: Amount of woven bone (red) and lamellar bone (green) in the thread region (—: HA side, ---: control side). Error bars indicate standard deviation (SD).

Regarding the contact rate of newly formed bone, no significant differences were detected between both groups over the whole experimental period. Contact rate increased during the first four weeks after screw insertion and stayed nearly constant for the remaining experimental period. However, normalizing contact rate to the available surface (= total surface minus surface of the implant occupied by HA particles), showed that significantly more new bone was in contact with the implant in the HA side at week 6 and 8 ($p = 0.002$ and $p = 0.002$) compared to the control side (Fig. 16).

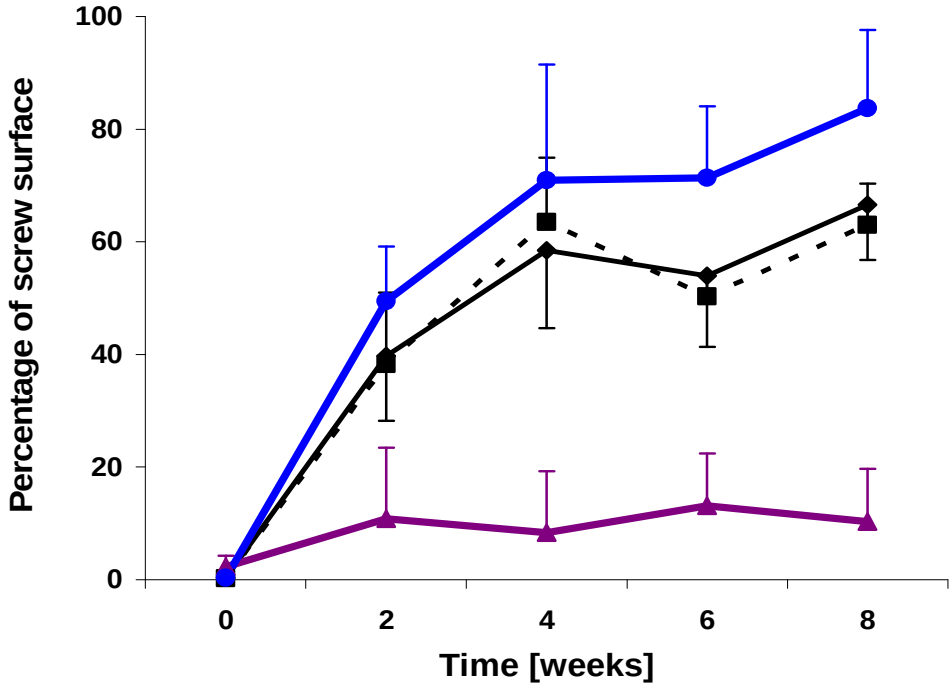

Fig. 16: Contact rate. Percentage of screw contour covered with HA particles (violet), newly formed bone (woven bone and lamellar bone added together, —: HA side, ---: control side) and newly formed bone normalized on the available surface after exclusion of the contour covered by HA particles (blue). Error bars indicate standard deviation (SD).

The amount of woven bone in contact with the implant increased significantly on both sides after two weeks ($p < 0.001$), while lamellar bone showed a significant and substantial increase two weeks later ($p < 0.001$). At week 6 and 8 after implantation, significantly more woven bone ($p = 0.002$ and $p = 0.004$) was in contact with the implant on the HA side, while the contact rate of lamellar bone was significantly higher on the control side ($p = 0.002$ and $p < 0.001$) (Fig. 17).

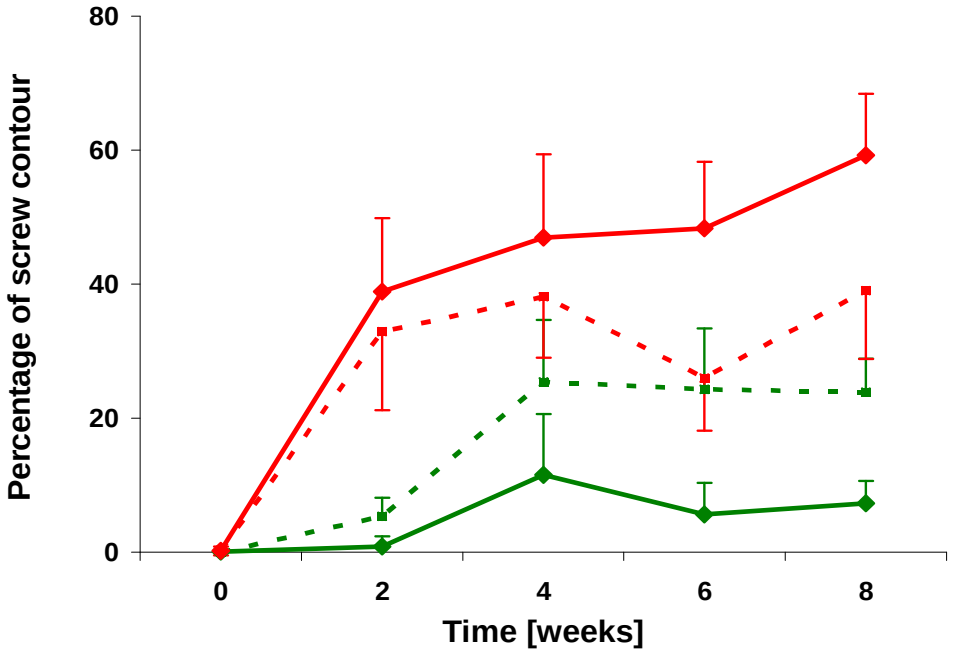

Fig. 17: Contact rate. Percentage of screw contour covered with woven bone (red) or lamellar bone (green) in the thread region (—: HA side, ---: control side). Error bars indicate standard deviation (SD).

One hour after implantation

In both groups (i.e. with and without HA particles), most of the cancellous material consisted of primary remodelled lamellar bone and mineralized epiphyseal cartilage. Due to implant insertion, trabeculae were broken and displaced between the screw threads (Fig. 18).

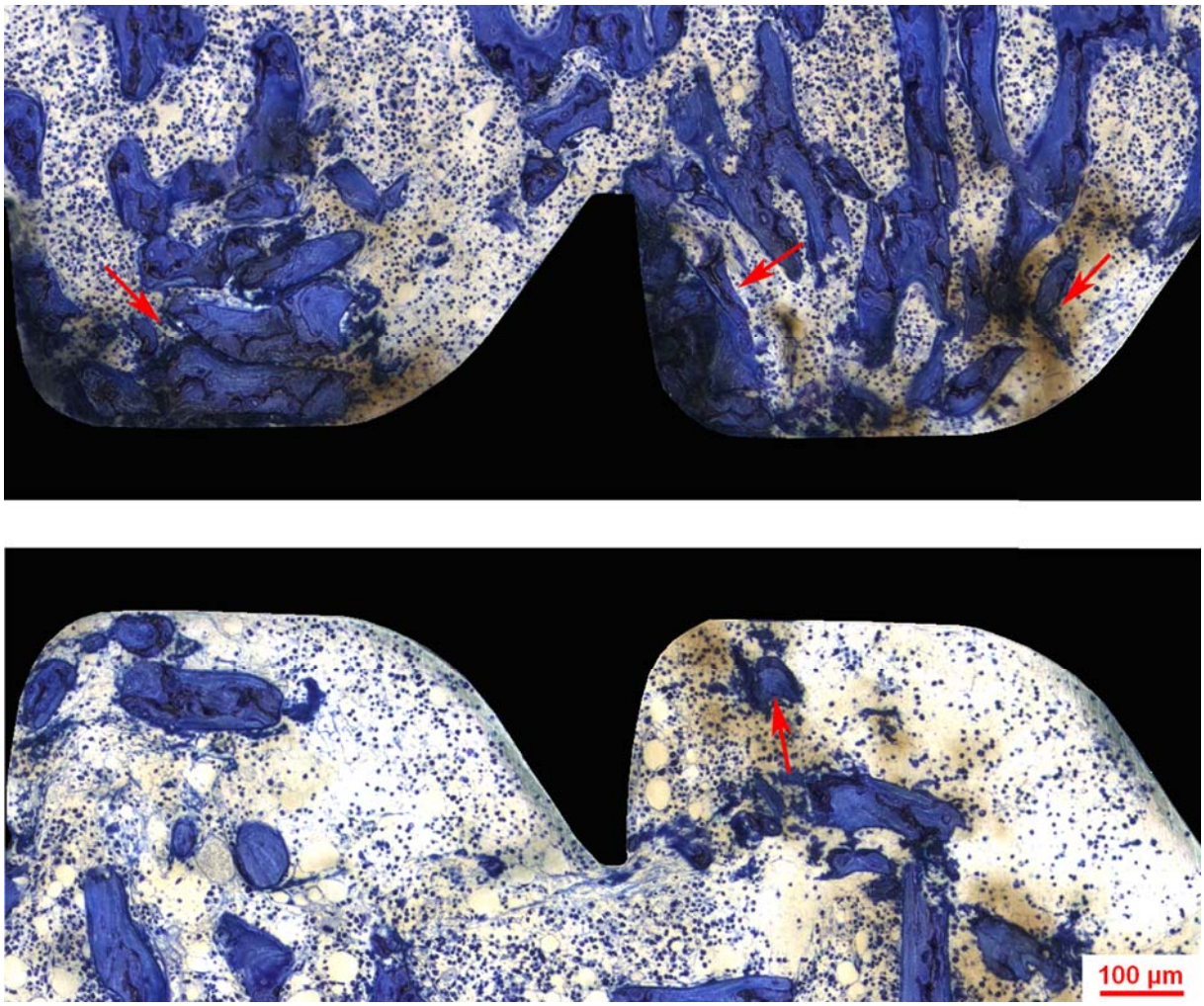

Fig 18: Control side (top and bottom): one hour after implantation. Preexisting cancellous bone (arrows) partially destroyed and displaced (toluidine blue, original magnification x100).

In the HA side, the HA particles were mostly concentrated between the threads of the screw. Due to the presence of HA, the cancellous bone was placed more marginal compared to the control side (Fig. 19).

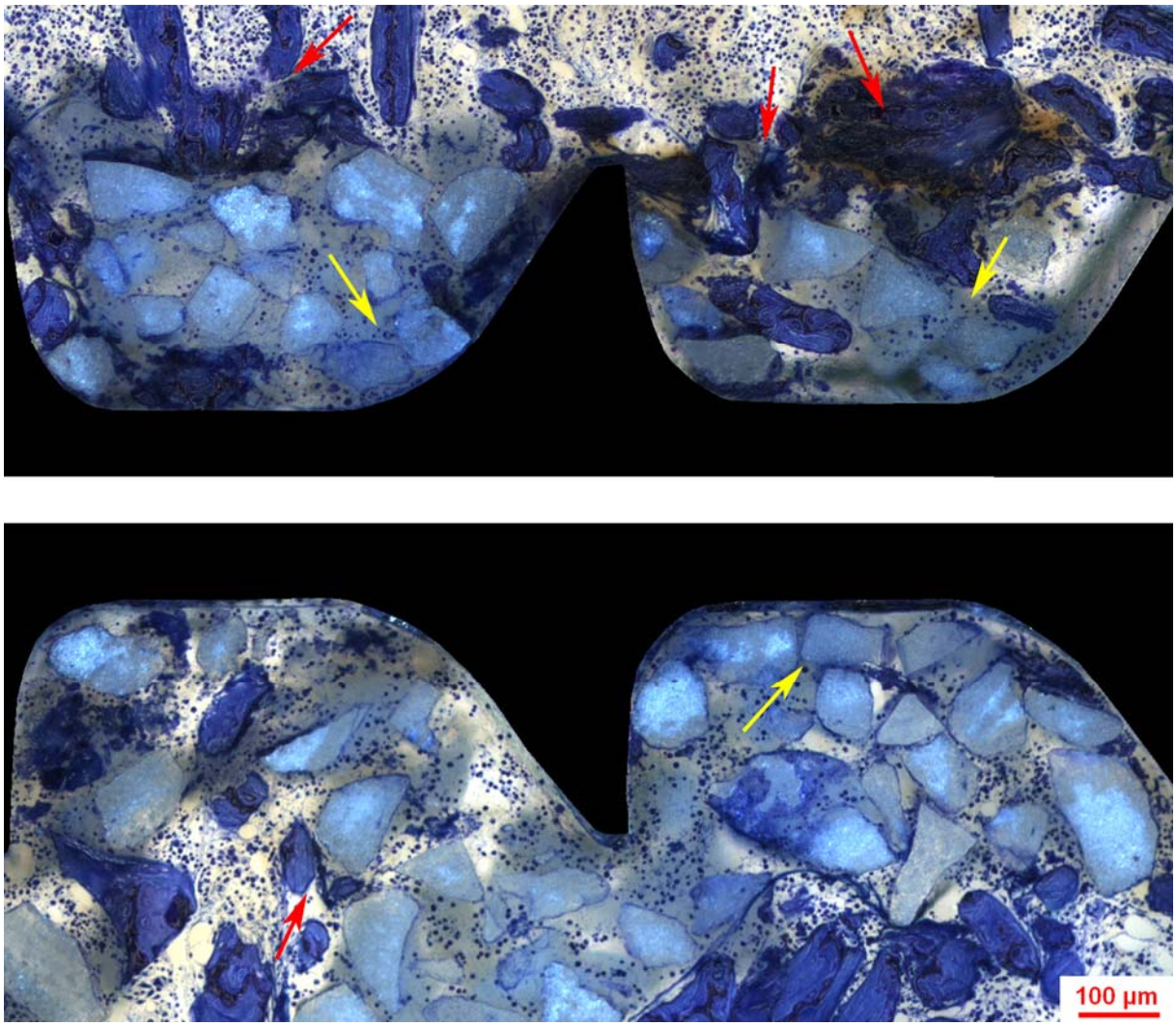

Fig. 19: HA side (top and bottom): one hour after implantation. Preexisting cancellous bone (red arrows) intensively destroyed and displaced. The inserted HA particles assembled closely to the implant surface (yellow arrows) (toluidine blue, original magnification x100).

No differences could be detected concerning the amount of newly formed bone due to the early time of bone healing in both sides (2.7% and 2.4%, control and HA side, respectively) (Fig. 14). Additionally, hardly any contact of newly formed woven bone

(0.2% and 0.2%, control and HA side, respectively), lamellar bone (0.0% and 0.1%, control and HA side, respectively) and HA particles (2.3%) with the implant surface was observed at this time point (Fig. 16, 17).

Two weeks after implantation

In the control side, a large amount of newly formed woven bone was observed around the implant. A small amount of newly formed lamellar bone surrounded primary remodelled bone and mineralized epiphyseal cartilage, both representing the cancellous bone material before screw implantation. Some trabeculae were connected to each other, forming a network and extending in direction of the implant. Bone-free implant surface was covered with loose connective or marrow tissue (Fig. 20).

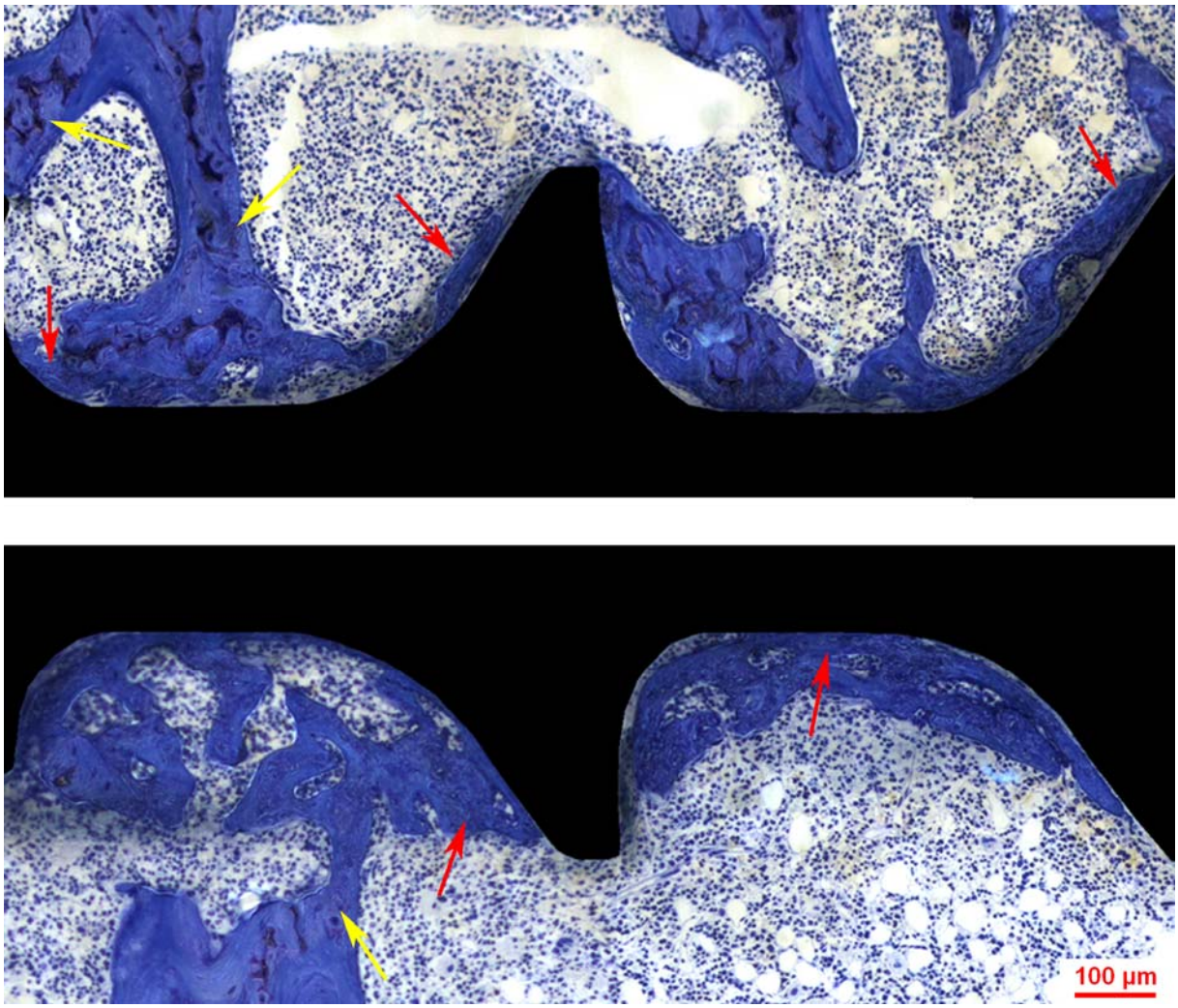

Fig. 20: Control side (top and bottom): two weeks after implantation. Newly formed woven bone in contact with implant surface (red arrows). Trabeculae with remnants of epiphyseal cartilage extending towards the implant (yellow arrows) (toluidine blue, original magnification x100).

In the HA side, newly formed woven bone filled up the interstitial space between the HA particles themselves and between HA particles and implant surface (Fig. 21).

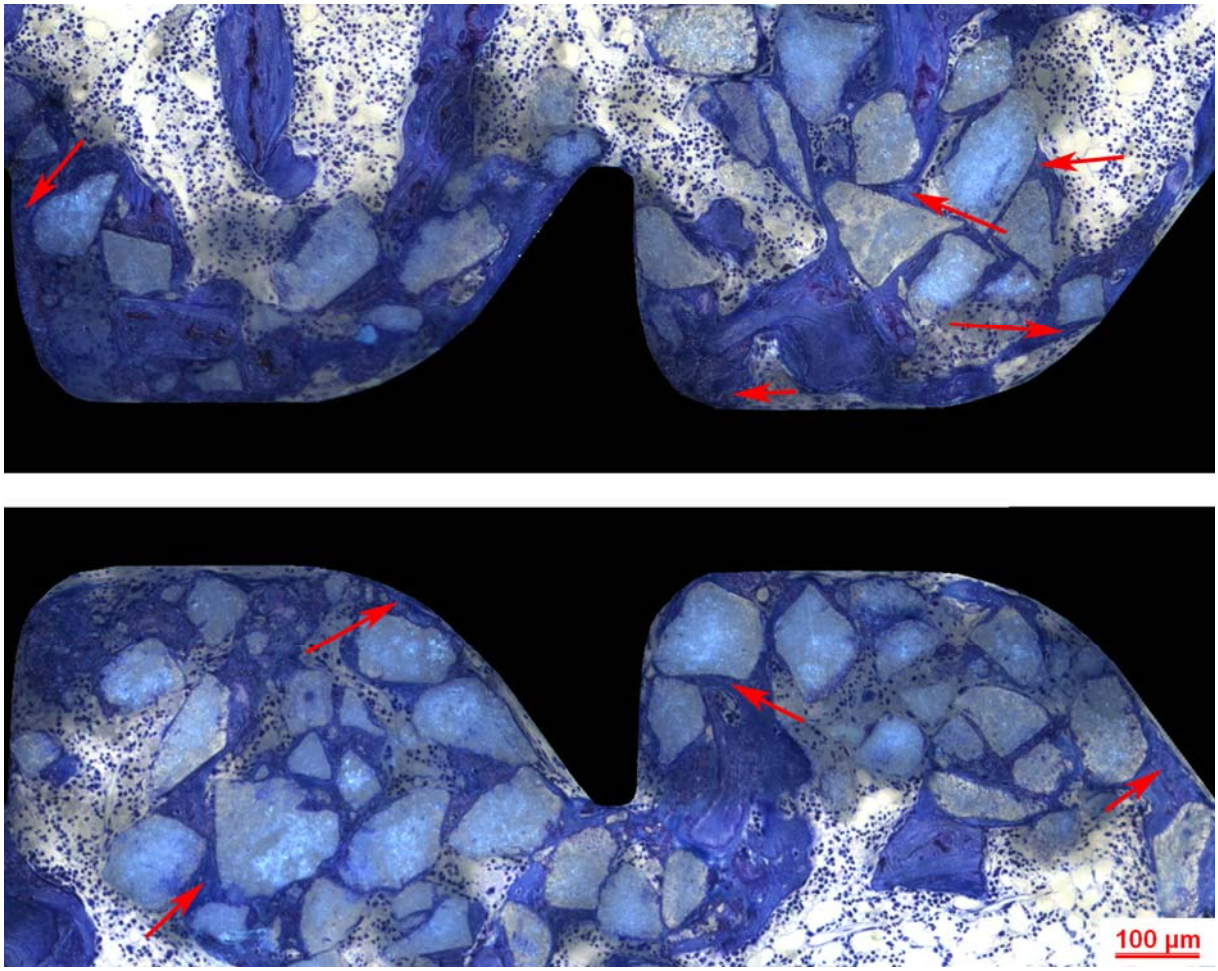

Fig. 21: HA side (top and bottom): two weeks after implantation. Newly formed woven bone outlining HA particles and implant surface (red arrows) (toluidine blue, original magnification x100).

In both sides woven bone amount increased significantly ($p < 0.001$) between one hour (2.0% and 2.0 %, control and HA side, respectively) and 2 weeks after implantation (20.8% and 26.3%) (Fig. 15). The amount of newly formed bone (woven and newly formed lamellar bone added together) was significantly but not substantially higher with HA (27.7%) compared to control (24.0%) ($p = 0.048$) (Fig. 14). With regard to contact rate, a significant increase ($p < 0.001$ and $p < 0.001$) of woven bone was observed, from 0.2% and 0.2% to 33.0% and 38.9%, control and HA side respectively. Instead, the amount of lamellar bone in contact with the implant surface did not show any significant change (Fig. 17). The contact rate of newly formed lamellar and woven bone together was not different ($p = 0.823$) in both sides (38.8% and 39.7%, control and HA side, respectively). HA particles represented a contact rate of 10.79% to the implant surface (Fig. 16).

Four weeks after implantation

Newly formed bone on the surface of existing cancellous bone showed increased thickness compared to the two weeks old specimens. In the control side, lamellar bone surrounded extensively woven bone and got in partial contact with the implant surface (Fig. 22).

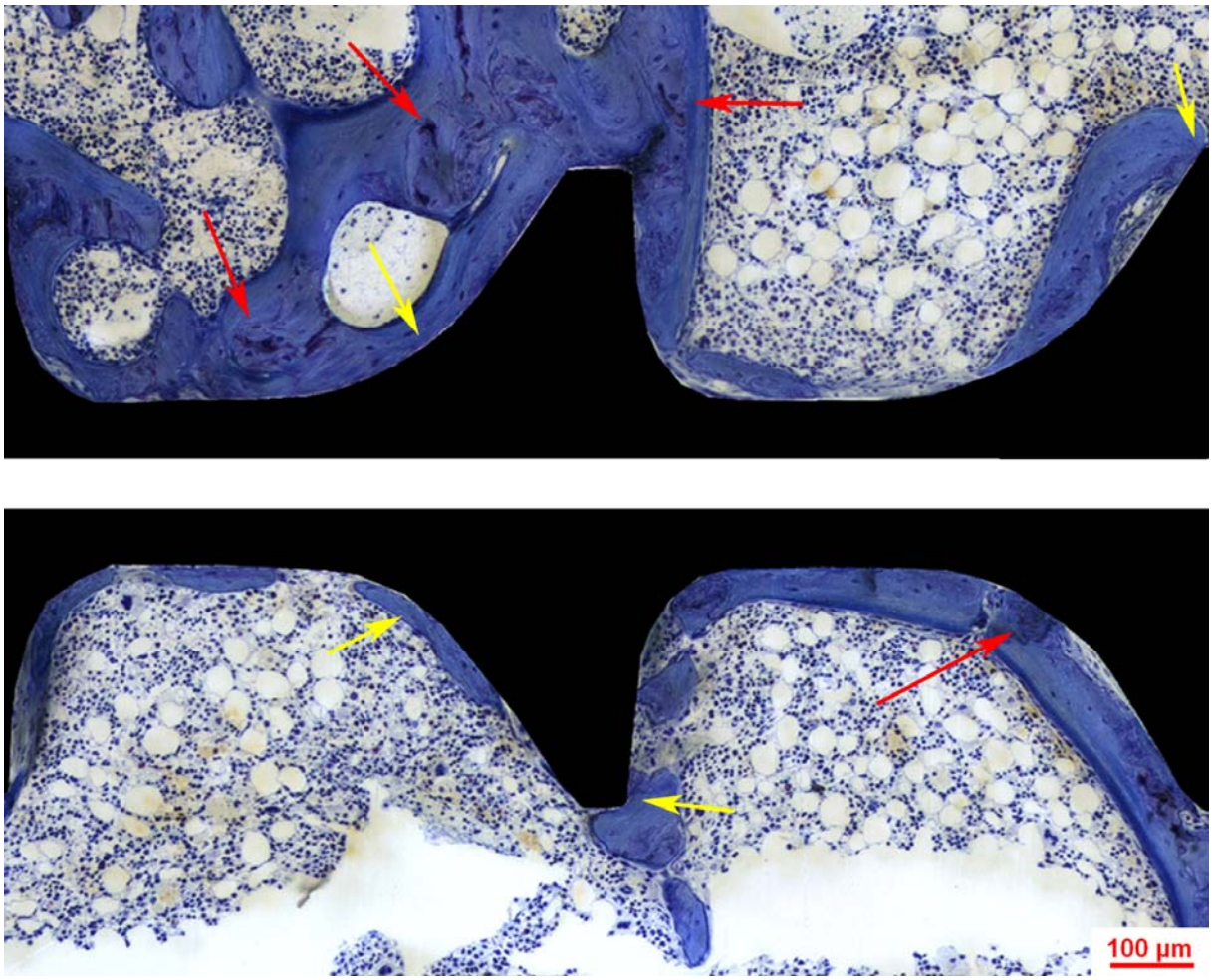

Fig. 22: Control side (top and bottom): four weeks after implantation. Newly formed lamellar bone, surrounding trabeculae with remnants of epiphyseal material and woven bone (red arrows), in partial contact with the implant surface (yellow arrows) (toluidine blue, original magnification x100).

In the HA group, woven bone was filling up the space between the HA particles. Woven bone and HA particles covered most of the implant surface. Instead, new lamellar bone was found on the outside of the peri-implant structure consisting of HA particles and woven bone and surrounded preexisting cancellous bone. Only few lamellae were in contact with the implant surface, especially in regions with less HA particles (Fig. 23).

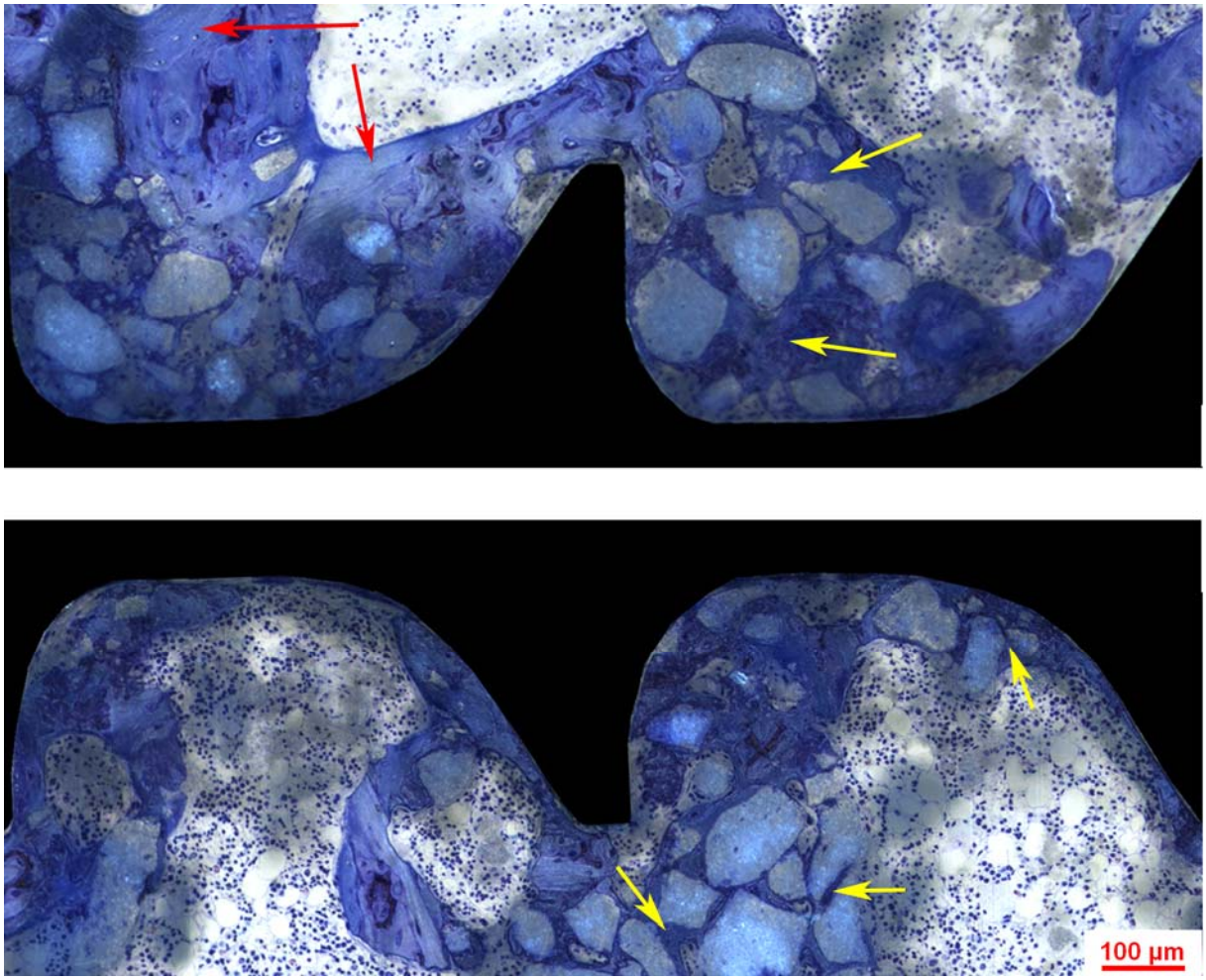

Fig. 23: HA side (top and bottom): four weeks after implantation. Thick layers of newly formed lamellar bone on the outside of the peri-implant structure formed by HA particles and woven bone. Lamellae surrounded HA, woven bone and epiphyseal material (red arrows). Space between HA filled up with newly formed woven bone (yellow arrows) (toluidine blue, original magnification x100).

When comparing the amount of newly formed bone, both sides showed a decrease of woven bone between two and four weeks after implantation, but only significantly in the control side ($p = 0.025$ and $p = 0.478$). While in the control side woven bone was reduced to less than half as much, i.e. from 20.8% to 9.5%, in the HA side the reduction was limited to approximately one quarter, i.e. going from 26.3% to 19.2%. During the same time frame, lamellar bone significantly increased ($p = 0.002$ and $p = 0.017$) in the control side from 3.2% to 7.8% and in the HA side from 1.4% to 4.4% (Fig. 15). Woven bone and newly formed lamellar bone added together was significantly higher ($p = 0.038$) with HA (23.6%) compared to the control side (17.3%) (Fig. 14).

Contact rate of newly formed lamellar bone exhibited a significant increase in both sides between two and four weeks ($p < 0.001$ and $p = 0.002$) (Fig. 17). In the control side, the contact-rate of lamellar bone was considerably higher (25.4%) compared to the HA side (11.6%) ($p = 0.005$). The contact of woven bone to the implant surface in the HA side started to be substantially higher compared to the control side (38.1% and 47.0%, respectively), however not yet significantly ($p = 0.113$). The contact of newly formed bone (lamellar and woven bone added together) was not significantly different ($p = 0.418$) in the control side (63.6%) compared to the HA side (58.5%). HA particles represented a contact rate of 8.34% (Fig. 16).

Six weeks after implantation:

In the control side, lamellar and woven bone covered the implant surface. Lamellar bone was also in contact with the surrounding cancellous bone via newly formed trabeculae. Uneven and thin layers of lamellar bone outlined the surface. Compared to two and four weeks after implantation, less bone was observed (Fig. 24).

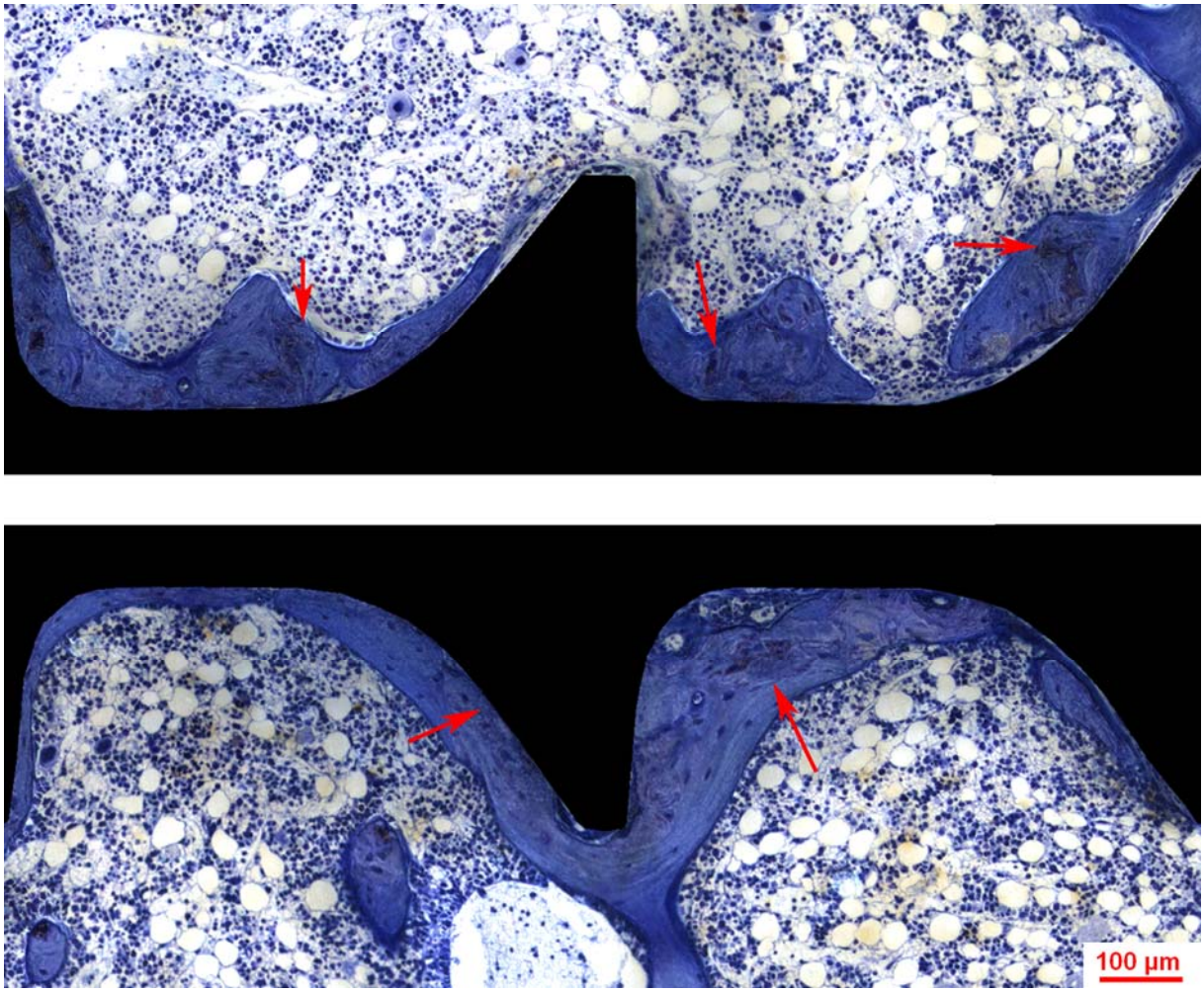

Fig. 24: Control side (top and bottom): six weeks after implantation. Newly formed bone surrounded nearly the whole surface of the implant. Residues of epiphyseal cartilage embedded in newly formed lamellar bone (red arrows) (toluidine blue, original magnification x100).

Nearly the whole space between HA particles and between HA and implant surface was filled with woven bone. The lamellar bone membrane, surrounding the outside of the HA ceramic and woven bone aggregation, became thicker, especially in the proximal part of the threaded region. The bone-free surface was usually covered with marrow tissue (Fig. 25).

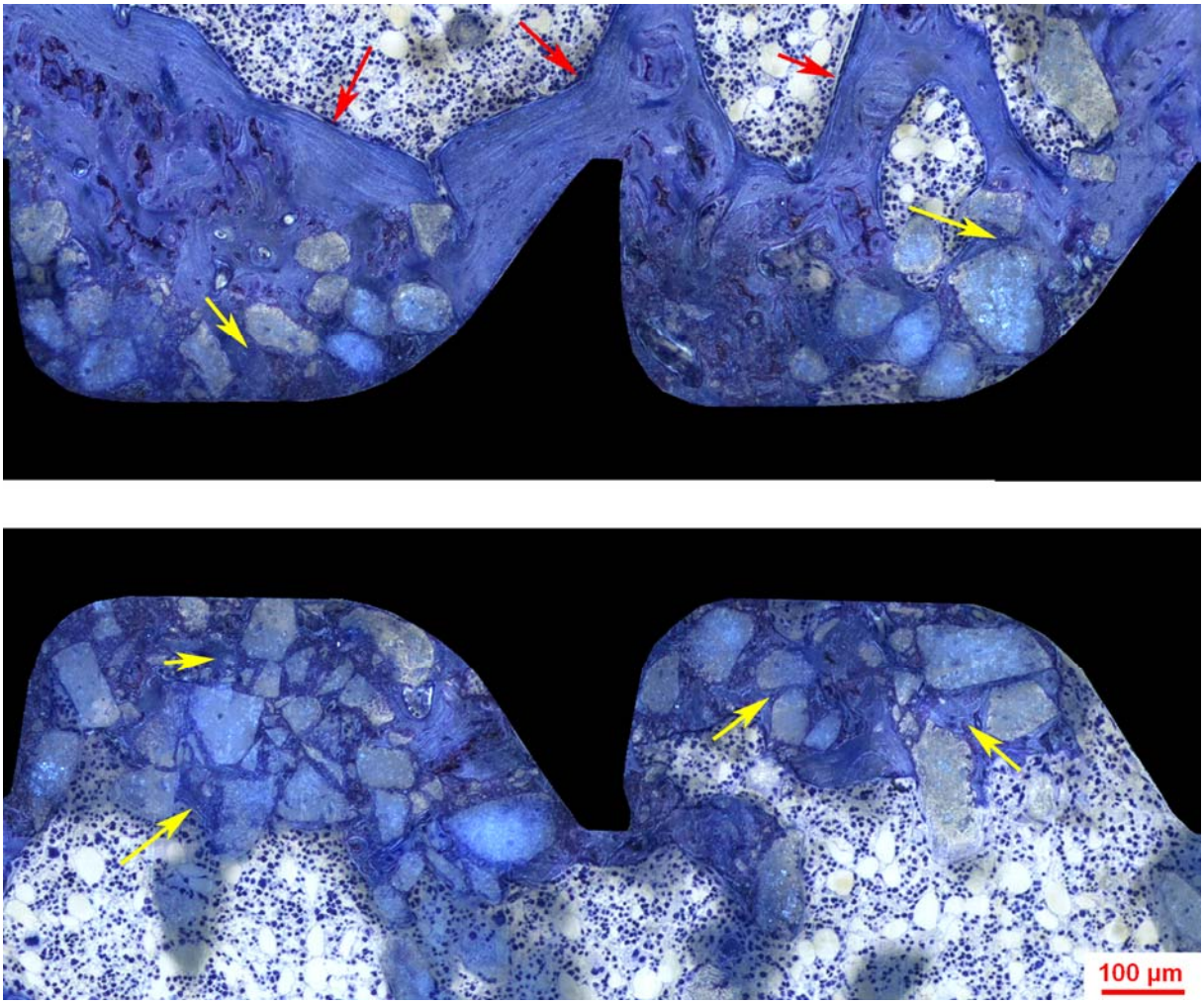

Fig. 25: HA side (top and bottom): six weeks after implantation. Space between HA filled with woven bone (yellow arrows). Top: implant surface covered with HA and woven bone. Newly formed lamellar bone as thick layers, surrounded HA particles, woven bone and remnants of epiphyseal material (red arrows). Bottom: hardly any lamellar bone visible except thin layers on the outside of HA (toluidine blue, original magnification x100).

Neither the amount of woven nor the amount of lamellar bone showed significant differences compared to four week old specimens. In the control side, the amount of lamellar bone showed no differences compared to the HA side (7.4% and 5.2%, respectively), whereas the amount of woven bone was significantly ($p < 0.001$) lower (4.9% and 19.6%, respectively) (Fig. 15). The amount of woven and lamellar bone added together was significantly higher ($p < 0.001$) in the HA side (24.3%) compared to the control side (12.0%) (Fig. 14).

While the contact rate of lamellar bone in the control side was not different between four and six weeks ($p = 0.702$), a decrease from 11.6% to 5.6% was detected in the HA side ($p = 0.237$). The opposite happened for woven bone: contact decreased from 38.1% down to 26.0% in the control side ($p = 0.066$), but no difference was detected in the HA side between four (47.0%) and six weeks (48.3%) after implantation ($p = 0.998$) (Fig. 17). The contact of newly formed bone (lamellar and woven bone together) decreased only significantly in the control side from 63.6% to 50.3% ($p = 0.028$) compared to the HA side from 58.5% to 54.0% ($p = 0.912$). HA particles had a percentage contact of 13.1% to the surface of the implant (Fig. 16).

Eight weeks after implantation

In the control side, woven bone was surrounded of newly formed lamellar bone. A thin and uniform layer of lamellar bone outlined the implant surface. Hardly any trabeculae could be observed in the cancellous region (Fig. 26).

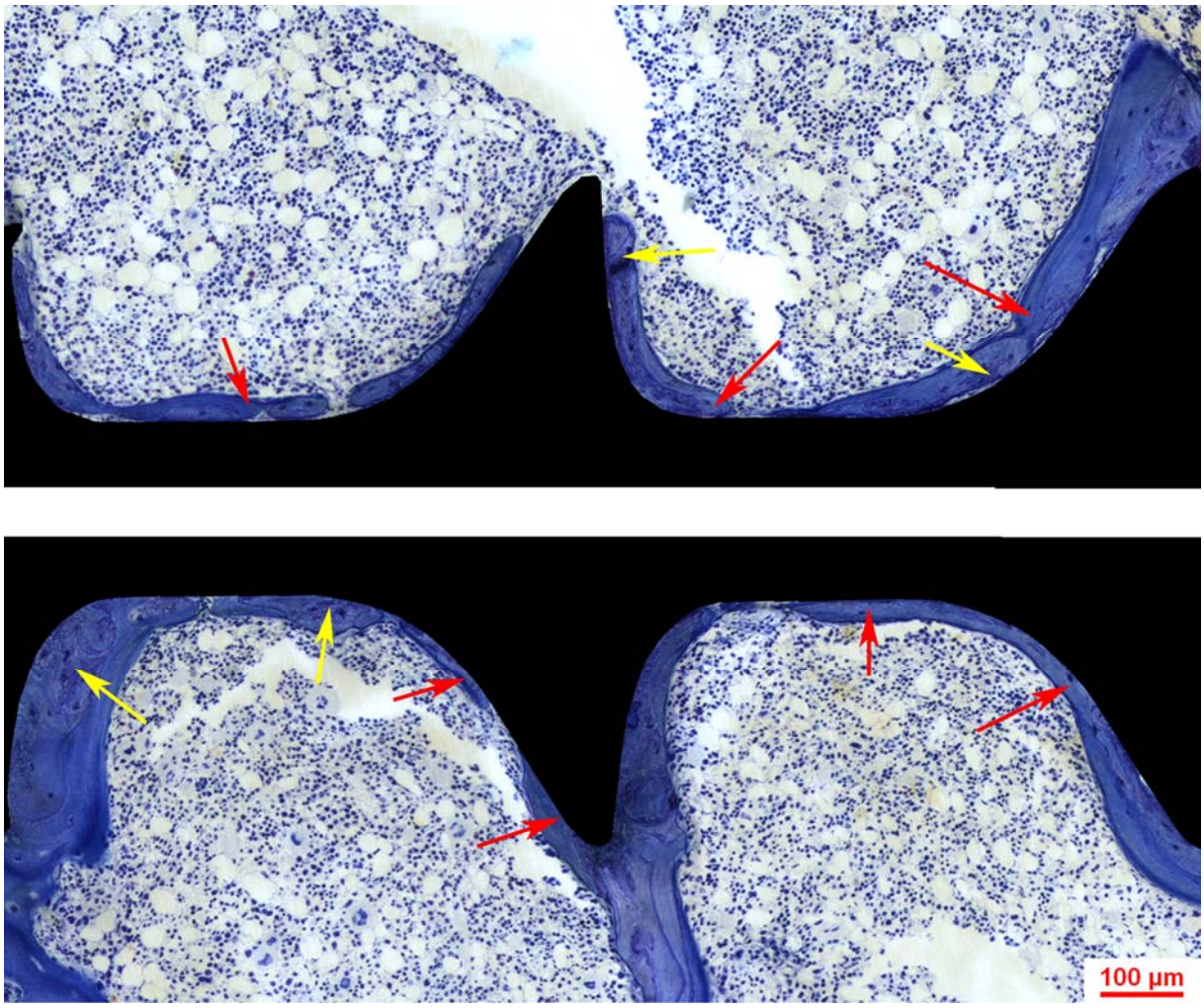

Fig. 26: Control side (top and bottom): eight weeks after implantation. Lamellar bone covering widely the implant surface (red arrows). Some woven bone embedded in lamellar bone (yellow arrows). Few trabeculae and low amount of bone in the thread region were visible (toluidine blue, original magnification x100).

In the HA side, the findings about woven bone were similar to those seen at six weeks after implantation. On the contrary, thick layers of lamellar bone were located on the outside of the peri-implant mantel consisting of HA particles and woven bone. Nearly the whole screw surface was covered with woven bone and HA particles (Fig. 27).

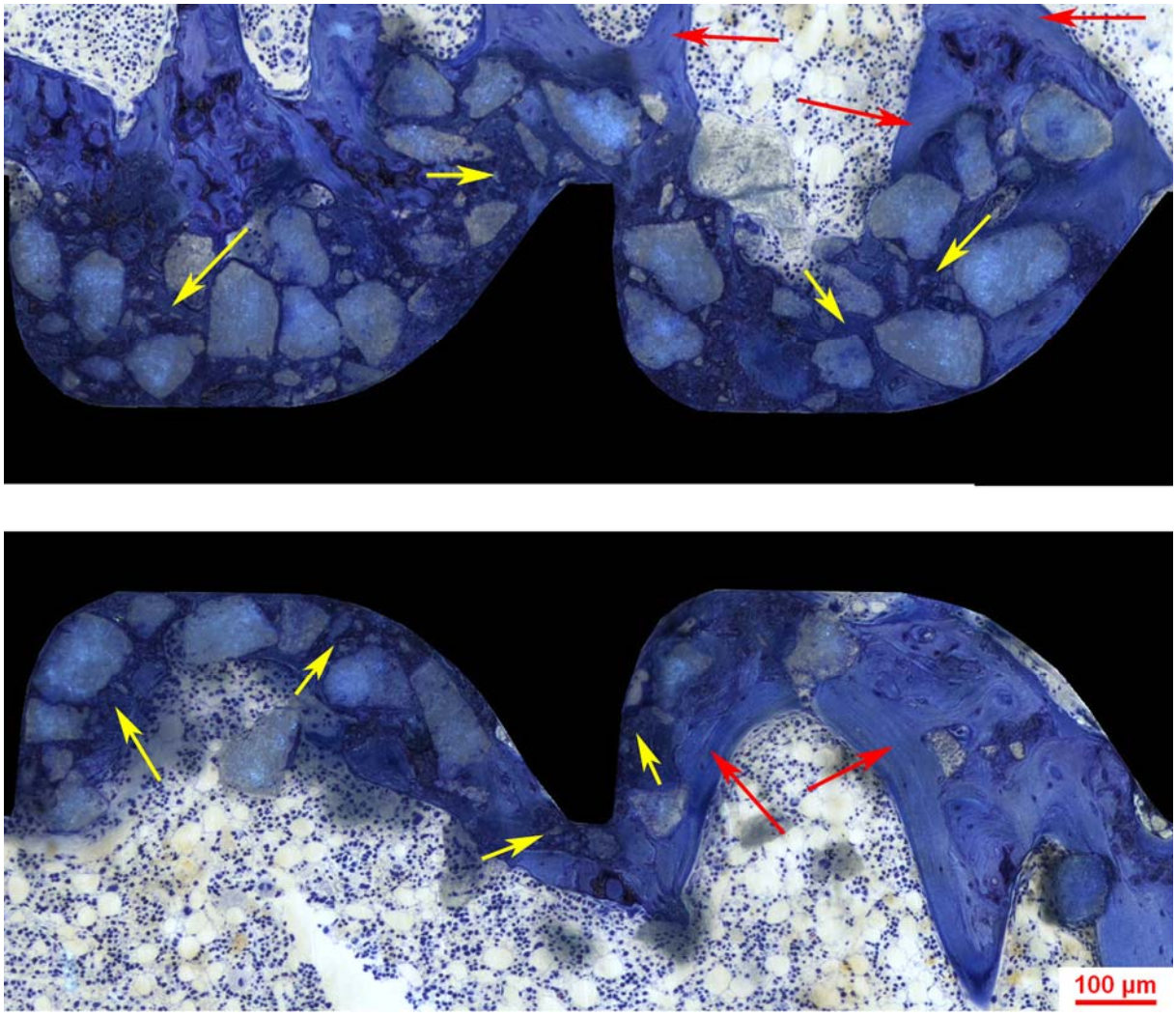

Fig. 27: HA side (top and bottom): eight weeks after implantation. Lamellar bone located marginally as a thick layer, which outlines HA particles and woven bone (red arrows). Space between HA completely filled with woven bone (yellow arrows) (toluidine blue, original magnification x100).

In both sides, the amount of woven bone remained constant at the same value as at four and six week after implantation The amount of lamellar bone showed a significant increase in both sides, from 7.4% to 10.2% ($p = 0.052$) in the control side and from 5.2% to 9.0% ($p < 0.001$) in the HA side (Fig. 15). The amount of newly formed bone was significantly higher ($p = 0.007$) in the HA side (28.3%) compared to the control side (17.5%) (Fig. 14).

The contact rate of woven bone showed a continuous, but not significant increase in the HA side up to 59.2% ($p = 0.174$), while in the control side the contact rate returned to almost the same value as at week 4 (39.1%) (Fig. 17). The contact rate of lamellar bone remained constant in both sides. The contact rate of lamellar and woven bone added together was not different between both sides at the end of the study (63.0 and 66.5%, control and HA side, respectively, $p = 0.456$). The contact rate of HA ceramic represented 10.3% (Fig. 16).

1.2. Longitudinal bone growth

Within eight weeks of the experimental period, a longitudinal bone growth of nearly 1,35 mm was measured between the screw-axis and the proximal growth plate of the tibia (Fig. 28). The growth was mainly linear with an approximate rate of 175 µm per week.

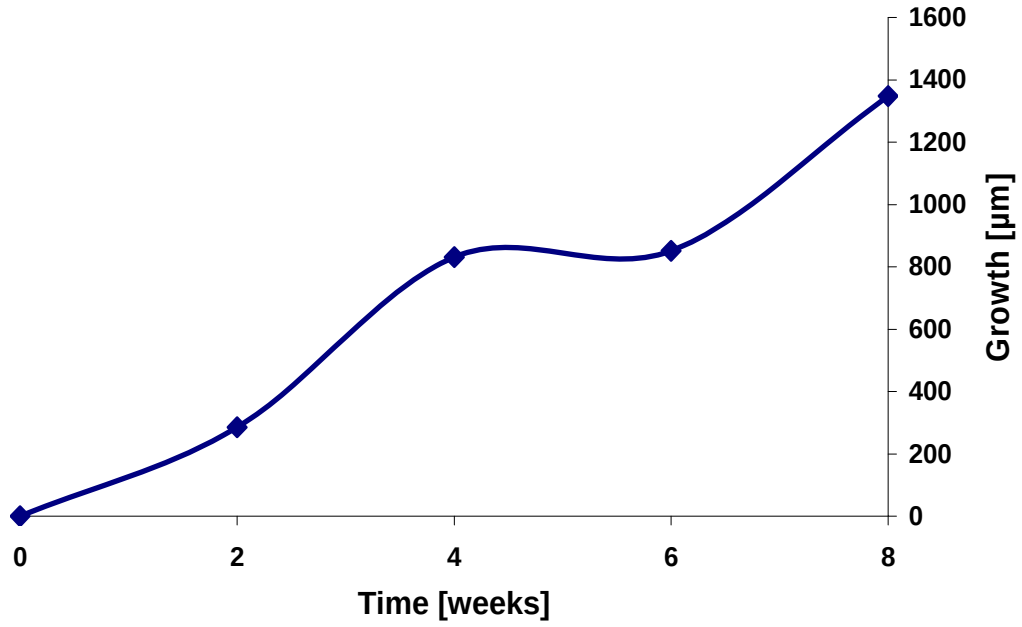

Fig. 28: Longitudinal bone growth during experimental period (rat age from week 16 till week 24).

2) Qualitative Analysis

Over the whole experimental period, a large amount of different bone marrow cell types with different morphologies i.e. lymphocytes, neutrophils, eosinophils and macrophages with their precursor cells were detected. As expected, the bone marrow of still growing, not yet adult rats (as used in our experiments) was very active and showed a dense cellular population at all time points.

As quantitatively assessed in sections stained with toluidine blue, woven bone formation was observed between HA particles and in direct contact with the implant. Woven bone formed a unique mass by connecting HA particles with each other. Bone marrow and few fat cells filled up the space between HA particles where woven bone was missing. At all time points bone marrow showed similar cellular activity: no specific or acute signs of inflammation or fibrosis were detected (Fig. 29).

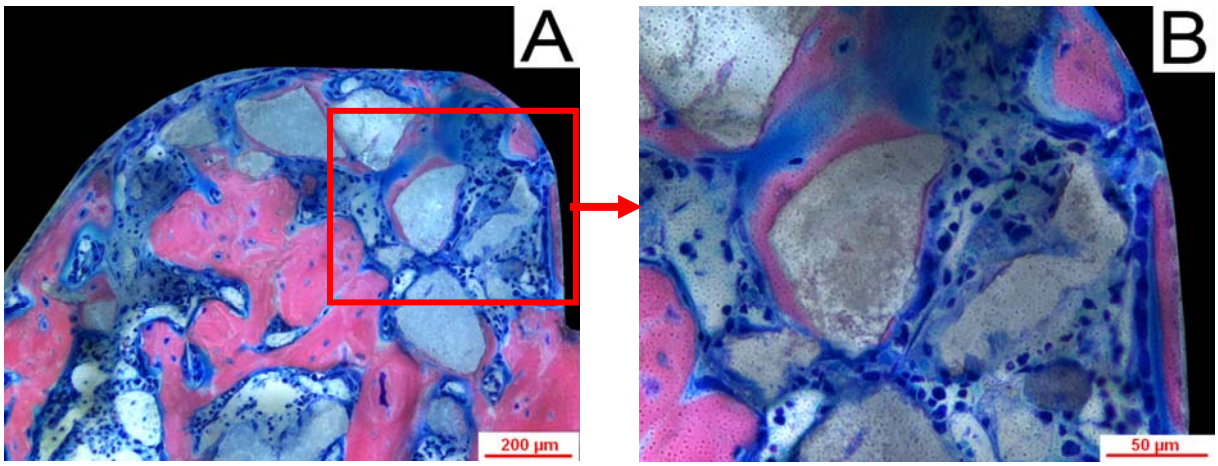

Fig. 29: Two weeks after implantation: HA side: Newly formed woven bone surrounding HA particles using them as a pattern (Giemsa/Eosin, original magnification x200 and x500).

A thin layer of non- or less mineralized bone matrix was observed, surrounding preexisting cancellous bone, starting two weeks after screw and HA insertion. Many active osteoblasts were detected concentrated two weeks after implantation. This fact corroborates the observation obtained with the quantitative analysis, whereby the largest amount of woven bone was produced in both sides in the first two weeks after implantation. The osteoblasts outlined bone surfaces as well as HA particles and produced the organic portion of bone tissue matrix (i.e. osteoid), whose structure defined by the collagen fibers was well organized. Remnants of epiphyseal cartilage material were also identified. They were surrounded by cancellous bone and newly formed bone material, as already visualized in the samples stained with toluidine blue (Fig. 30-33).

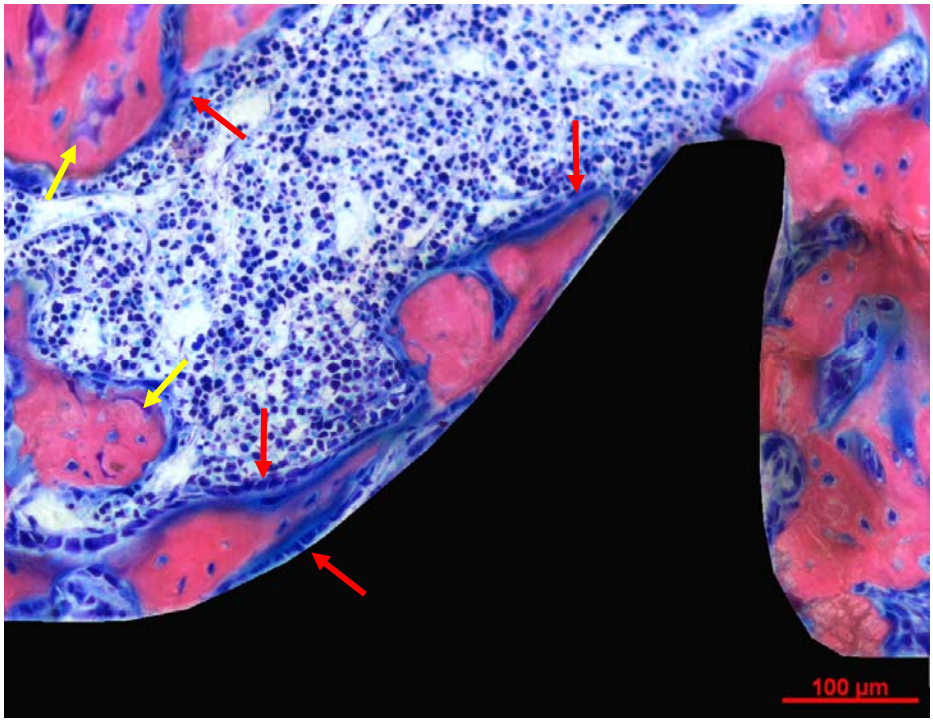

Fig. 30: Two weeks after implantation: control side: Osteoblasts outlining bone surfaces and producing osteoid (red arrows). Remnants of epiphyseal material (yellow arrow) surrounded both of preexisting cancellous bone and osteoid (Giemsa/Eosin, original magnification x200).

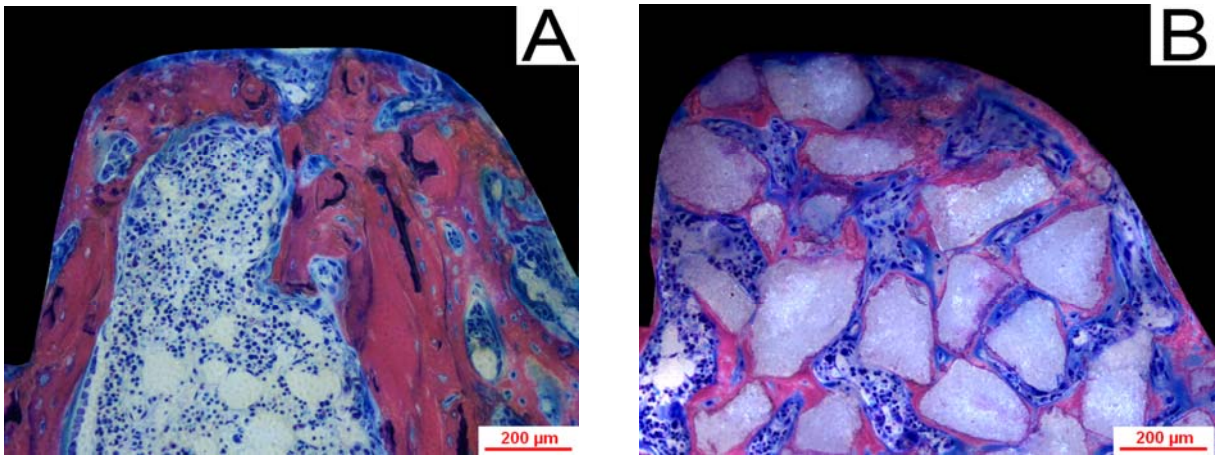

Fig. 31: Two weeks after implantation: control side (A) and HA side (B): Many active osteoblasts outlining HA and bone surfaces and producing osteoid. B: Preexisting cancellous bone displaced in the outer region of the ROI. HA particles between the threads of the screw. (Giemsa/Eosin, original magnification x200).

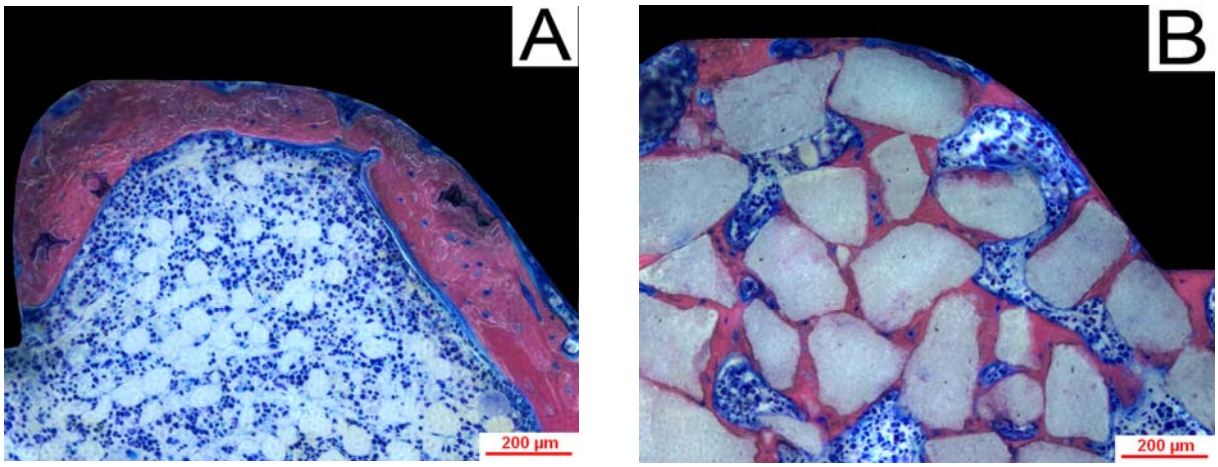

Fig 32: Four weeks after implantation: control side (A) and HA side (B): Less active osteoblasts visible compared to week 2. A: Layer of newly formed bone surrounding implant surface. Osteoid produced by osteoblasts along bone surfaces. B: Newly formed woven bone outlining HA and screw surface (Giemsa/Eosin, original magnification x200).

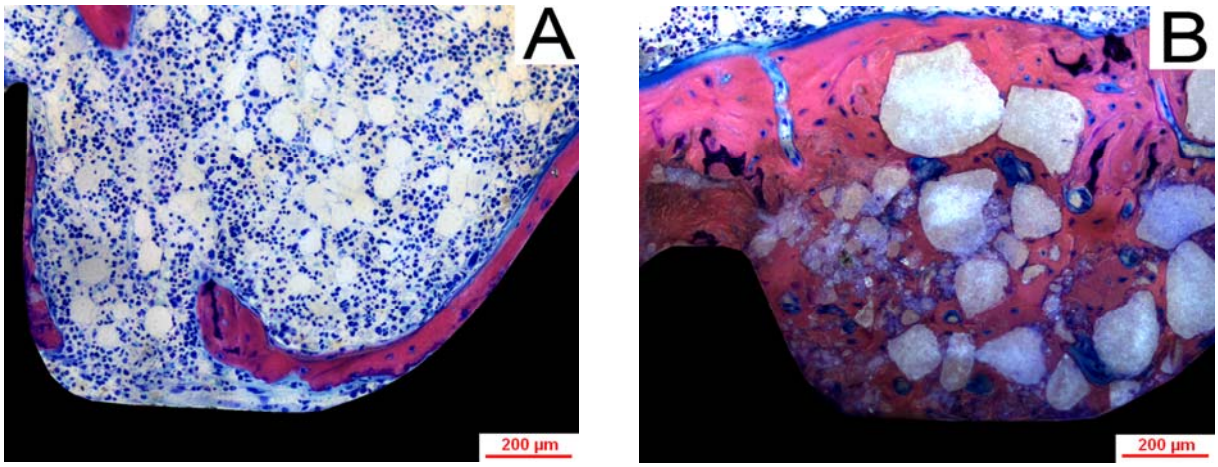

Fig. 33: Six weeks after implantation: In the control side (A) less amount of woven bone visible compared to the HA side (B), where woven bone filled up the whole space between HA particles. Less active osteoblasts visible, mostly outlined of the bone and still producing osteoid (Giemsa/Eosin, original magnification x200).

Remodelling units consisting of active osteoclasts and osteoblasts were also observed, especially at week 4, i.e. following the bone formation period. In the course of the healing process, preexisting cancellous bone, embedded epiphyseal material and woven bone were continuously remodelled into lamellar bone. While the osteoclasts resorbed bone tissue, in close proximity osteoblasts secreted new bone matrix (Fig. 34).

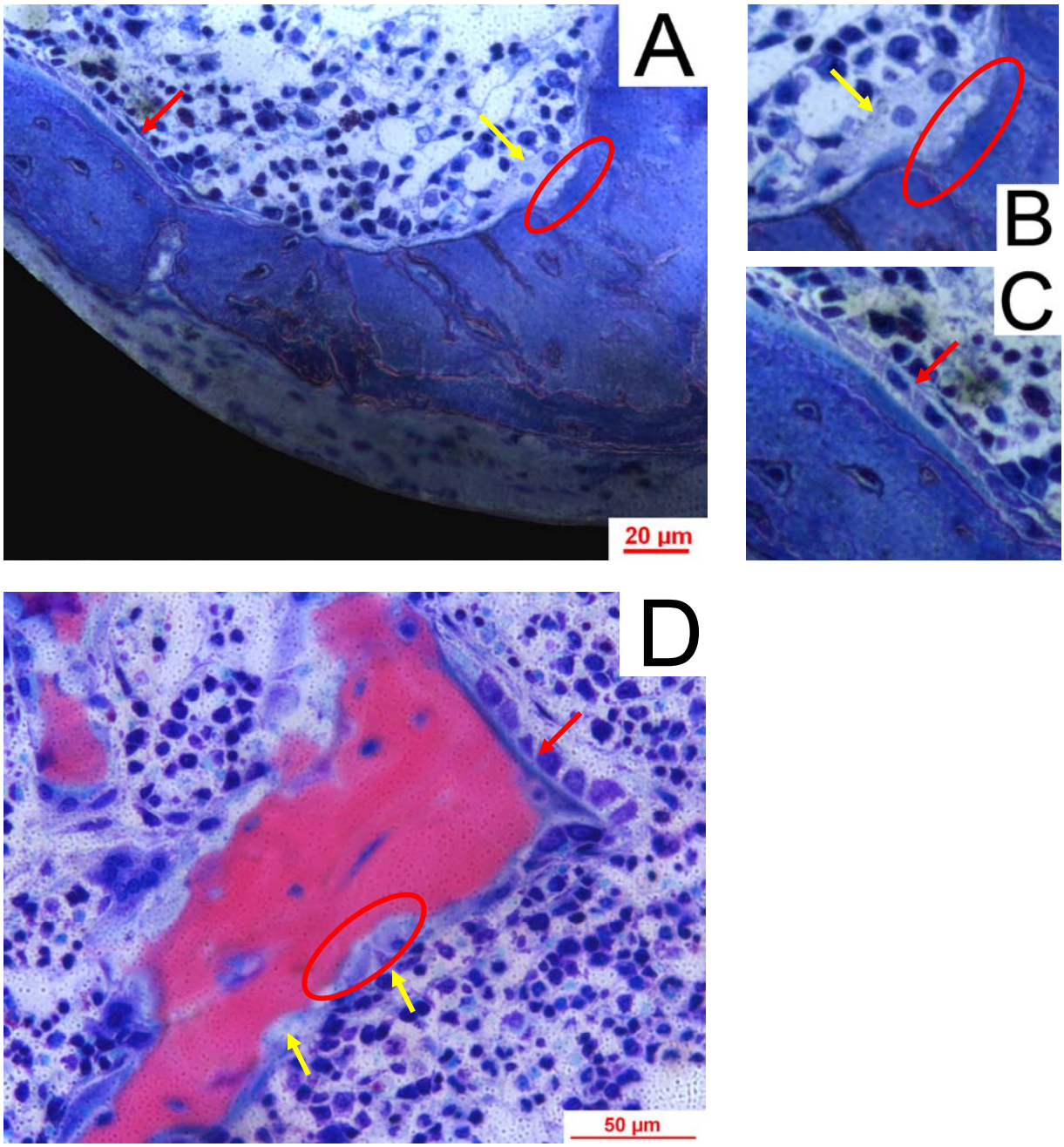

Fig. 34: Four weeks after implantation: Remodelling sequences: toluidine blue (A-C), Giemsa/Eosin (D): Osteoblasts secreting new bone matrix (red arrows: A, C, D). Osteoclasts (yellow arrows: B, D) performing bone resorption, visible through the ruffled border that seals the compartment for bone degradation (oval: A, B, D) (original magnification x200 and x500).

DISCUSSION

Loss of the surgical construct stability as a result of screw loosening is a well-known complication in osteoporotic patients. More than 50 % of proximal humerus fractures have fair or poor results because of screw loosening and pull-out from the humeral head [25]. Internal fixation of intertrochanteric fractures fails in 10% of cases because of cut-out of the lag screw from the cancellous bone of the femoral head [26]. The number of hip fractures, for example, that occur each year in the world has been estimated to be 1.66 million in 1990 and is predicted to rise to 6.26 million by the year 2050 [27,28]. The need of improved implant stability in osteoporotic bone is obvious and several methods have been developed to address this problem.

This study was designed to examine if HA particles were able to alter remodelling processes around implants inserted in osteoporotic bone. Based on an ovariectomized mature rat model, the results clearly demonstrated that the presence of HA particles inhibited resorption of woven bone starting between two weeks after screw implantation: A significantly denser peri-implant bone mantel was maintained and more extensive bone-implant contact was measured over the whole duration of the study, which are both critical parameters for improved implant osseointegration.

Data from pQCT-measurements verified the appropriateness of our rat model [29,30,31]. An osteoporotic state was successfully induced, corresponding to a mean decrease in bone mineral density of 33,9% at the distal femoral metaphyses four weeks after ovariectomy compared to age-matched sham-operated animals. This result stands in good agreement with previous publications [32]. In respect to our hypothesis, results from the histologic analysis evidenced that after the initial bone formation phase for about two weeks, the amount of woven bone surrounding the screw decreased in both sides (i.e. with and without HA particles) as a typical

consequence of bone resorption processes and increased bone turnover following ovariectomy [33,34]. The bone loss affected pre-existing cancellous bone as well as newly formed bone trabeculae [14]. However, this decrease was significantly reduced in the HA side: more than twice of the amount of woven bone remained in the peri-implant region until the end of the experimental period compared to the control side. Moreover, HA particles also induced more contact of new bone with the implant surface. Despite the substantial space occupied by the inserted HA particles, the total percentage of screw perimeter covered by bone tissue was nearly the same amount in both sides at all time points. When we normalized the contact rate results to the available surface perimeter, new bone had more contact to the implant surface in the HA side compared to the control side. Hence, not only did HA particles induce more bone formation but they apparently promoted more bone deposition directly on the implant surface till the end of the experimental period. These results corroborates with previous studies where the good biocompatibility as well as the osseoconductive and osseoinductive properties of HA particles in rat bone were assessed [35,36,37].

The novelty of our study concerning the use of HA is twofold: besides testing a new, simple technique that took advantage of the known bioactive properties of HA, we also monitored the effect of those particles at different time points during the bone healing processes in an osteoporotic rat model. Instead of performing a complex coating process [24,29], small HA particles were inserted in a predrilled hole before implant placement. The absence of any signs of inflammation suggested that this surgical technique could be quite a conceivable alternative in clinical settings too. In previous studies the effect of HA was mainly tested on coated implants using normal, healthy animal models (i.e. lacking the bone turnover affected by osteoporosis) [38,39,40], or in osteoporotic animals but only at one time focussing on long-term

effects, disregarding the bone formation processes in the healing phase after surgery [41,42].

Previous studies have reported transient effects of HA in coatings: its stimulatory effect at early time periods diminished with time. Mechanical tests on HA-coated implants were consistent with these findings [40]. Our data also demonstrate that more bone was formed during the first two weeks of the healing phase (i.e. bone formation phase), but HA particles seemed to affect more distinctively the remodelling phase leaving more woven bone in the peri-implant region. The rather continuous and linear bone layer covering the implant in the control side might be more exposed and vulnerable to osteoclastic activity. By contrast, woven bone embedded between HA particles could be guarded against resorption by partially blocking access to larger cells like osteoclasts.

The fate of this additional amount of woven bone after the experimental period is not known. In rat models the remodelling processes are usually in an advanced stage at eight week after surgical procedure. However, the reduced amount of lamellar bone in the HA side points to a delay in this biological cascade. In the control side, remodelling processes were observed around the implant surface and around pre-existing trabeculae, whereas in HA side newly formed lamellar bone was missing around implant surface [43,44,45] and between HA particles. Most of the lamellar bone was detected around the structure consisting of screw, woven bone and HA particles.

Regarding the functionality of the effect induced by HA particles, unfortunately the experimental design in this study did not permit to carry out mechanical tests on paired samples, which should be included in future studies. Moreover, the location used for implantation, i.e. cancellous versus cortical bone, will affect the course of

osseointegration, because trabeculae offer a larger surface compared to the cortex [8,46]. To avoid mixed effects, we limited our analysis to the threaded part of the screw and discarded the tip, so that at all time-points only cancellous bone would be in contact with the surface. Due to normal axial growth of the limb in still growing mature rats [47-52], screw moved distally and at later time points (six and eight weeks) most of the tips were anchored in the cortex.

In summary, this study demonstrated that non-resorbable HA particles were able to maintain significantly peri-implant bone material in osteoporotic trabecular bone. The presence of HA particles affected remodelling processes and improved osseointegration. This effect may play an important role in the prevention of implant loosening and cut-outs in clinical cases.

REFERENCES

[1] Epidemiology of osteoporosis, http://www.osteoporose.de/osteoporose_Wissen/Epidemiologie.de, Munich 2008

[2] National Osteoporosis Foundation. Fast Facts. Available at: http://www.nof.org/osteoporosis/diseasefacts.htm, National Osteoporosis Foundation. Washington (DC);2008

[3] National Osteoporosis Foundation. America`s bone health: the state of osteoprosis and low bone mass in our nation. Available at: http://www.nof.org/advocacy/prevalence/index.htm, National Osteoporosis Foundation. Washington (DC);2008

[4] **Lippuner** K, Golder M, Greiner R. Epidemiology and direct medical costs of osteoporotic fractures in men and women in Switzerland. Osteoporos.Int. 2005;16:8-17.

[5] **Cornell** CN. Internal fracture fixation in patients with osteoporosis. J.Am.Acad.Orthop.Surg. 2003;11:109-119.

[6] National Osteoporosis Foundation. Clinician's guide to prevention and treatment of osteoporosis. National Osteoporosis Foundation. Washington (DC);2008

[7] **Kim** WY, Han CH, Park JI, Kim JY. Failure of intertrochanteric fracture fixation with a dynamic hip screw in relation to pre-operative fracture stability and osteoporosis. Int.Orthop. 2001;25:360-362.

[8] **Stepan** JJ, Pospichal J, Presl J, Pacovsky V. Bone loss and biochemical indices of bone remodeling in surgically induced postmenopausal women. Bone 1987;8:279-284.

[9] **Yamazaki** M, Shirota T, Tokugawa Y, Motohashi M, Ohno K, Michi K, Yamaguchi A. Bone reactions to titanium screw implants in ovariectomized animals. Oral Surg.Oral Med.Oral Pathol.Oral Radiol.Endod. 1999;87:411-418.

[10] **Duarte** PM, Cesar-Neto JB, Sallum AW, Sallum EA, Nociti FH, Jr. Effect of estrogen and calcitonin therapies on bone density in a lateral area adjacent to implants placed in the tibiae of ovariectomized rats. J.Periodontol. 2003;74:1618-1624.

[11] **Shirota** T, Tashiro M, Ohno K, Yamaguchi A. Effect of intermittent parathyroid hormone (1-34) treatment on the bone response after placement of titanium implants into the tibia of ovariectomized rats. J.Oral Maxillofac.Surgery 2003;61:471-480.

[12] **Narai** S, Nagahata S. Effects of alendronate on the removal torque of implants in rats with induced osteoporosis. Int.J.Oral Maxillofac.Implants. 2003;18:218-223.

[13] **Tokugawa** Y. Effects of bisphophonate on bone reaction after placement of titanium implants in tibiae of ovariectomized rats. Int.J.Oral Maxillofac.Implants. 2003;18:66-74.

[14] **Motohashi** M, Shirota T, Tokugawa Y, Ohno K, Michi K, Yamaguchi A. Bone reactions around hydroxyapatite-coated implants in ovariectomized rats. Oral Surg. Oral Med.Oral Pathol.Oral Radiol.Endod. 1999;87: 145-152.

[15] **Hasegawa** T, Inufusa A, Imai Y, Mikawa Y, Lim TH, An HS. Hydroxyapatite-coating of pedicle screws improves resistance against pull-out force in the osteoporotic canine lumbar spine model: a pilot study. Spine J. 2005;5:239-243.

[16] **Hayashi** K, Fotovati A, Ali SA, Oda K, Oida H, Naito M. Prostaglandin EP4 receptor agonist augments fixation of hydroxyapatite-coated implants in a rat model of osteoporosis. J.Bone Joint Surg.Br. 2005;87:1150-1156.

[17] **Blouin** S, Moreau MF, Weiss P, Daculsi G, Basle MF, Chappard D. Evaluation of an injectable bone substitute (betaTCP/hydroxyapatite/hydroxy-propyl-methyl-cellulose) in severely osteopenic and aged rats. J.Biomed.Mater.Res. A 2006;78:570-580.

[18] **Hing** KA, Best SM, Tanner KE, Bonfield W, Revell PA. Biomechanical assessment of bone ingrowth in porous hydroxyapatite. J.Mater.Sci.Mater.Med. 1997;8:731-736.

[19] **van Blitterswijk** CA, Hesseling SC, Grote JJ, Koerten HK, de Groot K. The biocompatibility of hydroxyapatite ceramic: a study of retrieved human middle ear implants. J.Biomed.Mater.Res. 1990;24:433-453.

[20] **Liebendorfer** A, Troster S. Hydroxyapatite ceramics in clinical application. Histological findings in 23 patients. Unfallchirurgie 1997;23:60-68.

[21] **Schaller** P. Spongiöse Hydroxylapatitkeramik (Endobon) zur Auffütterung von Knochenhöhlen am Hand- und Fusskelett. Osteo.Int. 1994;2:128-134.

[22] **Werber** KD, Brauer RB, Weiss W, Becker K. Osseous integration of bovine hydroxyapatite ceramic in metaphyseal bone defects of the distal radius. J.Hand Surg.[Am.] 2000;25:833-841.

[23] **Bauer** HJ, Bauer M, Dingeldein E. Zusammensetzung und Aufbau einer porösen Hydroxylapatitkeramik biologischer Herkunft. Osteo.Int. 1994;2:106-110.

[24] **Fini** M, Giavaresi G, Greggi T, Martini L, Aldini NN, Parisini P, Giardino R. Biological assessment of the bone-screw interface after insertion of uncoated and hydroxyapatite-coated pedicular screws in the osteopenic sheep. J.Biomed.Mater.Res.A 2003;66:176-183.

[25] **Kristiansen** B, Christensen SW. Plate fixation of proximal humeral fractures. Acta Orthop.Scand. 1986;57:320-323.

[26] **Baumgaertner** MR, Curtin SL, Lindskog DM, Keggi JM. The value of the tip-apex distance in predicting failure of fixation of peritrochanteric fractures of the hip. J.Bone Joint Surg.Am. 1995;77:1058-1064.

[27] **Cooper** C, Campion G, Melton LJ. Hip fractures in the elderly: a world-wide projection. Osteoporos.Int. 1992;2:285-289.

[28] **Johnell** O, Kanis J. Epidemiology of osteoporotic fractures. Osteoporos.Int. 2005;16:3-7.

[29] **Pan** J, Shirota T, Ohno K, Michi K. Effect of ovariectomy on bone remodeling adjacent to hydroxyapatite-coated implants in the tibia of mature rats. J.Oral Maxillofac.Surg. 2000;58:877-882.

[30] **Wronski** TJ, Schenck PA, Cintron M, Walsh CC. Effect of body weight on osteopenia in ovariectomized rats. Calcif.Tissue Int. 1987;40:155-159.

[31] **Duarte** PM, Neto JBC, Gonçalves PF, Sallum EA, Nociti FH. Estrogen deficiency affects bone healing around titanium implants: a histometric study in rats. Implant.Dent. 2003;12:340-346.

[32] **Laib** A, Kumer JL, Majumdar S, Lane NE. The temporal changes of trabecular architecture in overiectomized rats assessed by MicroCT. Osteoporos.Int 2001;12:936-941.

[33] **Miller** SC, Wronski TJ. Long-term osteopenic changes in cancellous bone structure in ovariectomized rats. Anat.Rec. 1993;236:433-441.

[34] **Wronski** TJ, Dann LM, Horner SL. Time course of vertebral osteopenia in ovariectomized rats. Bone 1989;10:295-301.

[35] **Herr** G, Küsswetter W, Thielemann FW. Granuläre Hydroxylapatitkeramiken als Wirkstoffdepot für osteoinduktive Faktoren. Osteo.Int. 1994;2:148-152.

[36] **Tatatarenko-Kozmina** TY, Denisov-Nikol`skii YI, Volozhin AI, Doktorov AA, Mal`ginov NN, Krasnov AP. Effect of hydroxyapatite as a component of biostable composites on population and proliferation of mesenchymal stem cells. Bull.Exp.Biol.Med. 2007;143:519-523.

[37] **Fu** Q, Zhou N, Huang W, Rahaman MN, Wang D, Zhang L, Li H. In vitro study on different cell response to spherical hydroxyapatite nanoparticles. J.Biomater.Appl. 2008 [Epup ahead of print].

[38] **Tsukeoka** T, Suzuki M, Ohtsuki C, Tsuneizumi Y, Miyagi J, Sugino A, Inoue T, Michihiro R, Moriya H. Enhanced fixation of implants by bone ingrowth to titanium fiber mesh: effect of incorporation of hydroxyapatite powder. J.Biomed.Mater.Res.B Appl.Biomater. 2005;75:168-176.

[39] **Meirelles** L, Albrektsson T, Kjellin P, Arvidsson A, Frenke-Stenport V, Andersson M, Currie F, Wennerberg A. Bone reaction to nano hydroxyapatite modified titanium implants placed in a gap-healing model. J.Biomed.Mater.Res. A 2008 [Epup ahead of print].

[40] **Soballe** K. Hydroxyapatite ceramic coating for bone implant fixation. Mechanical and histological studies in dogs. Acta Orthop.Scand.Suppl. 1993;255:1-58.

[41] **Aldini** NN, Fini M, Giavaresi G, Giardino R, Greggi T, Parisini P. Pedicular fixation in the osteoporotic spine: a pilot in vivo study on long-term ovariectomized sheep. J.Orthop.Res. 2002;20:1217-1224.

[42] **Hara** T, Hayashi K, Nakashima Y, Kanemaru T, Iwamoto Y. The effect of hydroxyapatite coating on the bonding of bone titanium implants in the femora of ovariectomised rats. J.Bone Joint Surg. Br. 1999;81:705-709.

[43] **Wronski** TJ, Dann LM, Scott KS, Cintron M. Long-term effect of ovariectomy and aging on the rat skeleton. Calcif.Tissue Int. 1989;45:260-366

[44] **Turner** RT, Riggs BL, Spelsberg TC. Skeletal effects of estrogen. Endocr.Rev. 1994;15:275-300.

[45] **Peter** B, Gauthier O, Laib S, Bujoli B, Guicheux J, Janvier P, van Lenthe GH, Muller R, Zambelli PY, Bouler JM, Pioletti DP. Local delivery of bisphosphonate from coated orthopedic implants increases implants mechanical stability in osteoporotic rats. J.Biomed.Mater.Res.A 2006;76:133-143.

[46] **Vaananen** HK, Harkonen PL. Estrogen and bone metabolism. Maturitas. 1996;23 (suppl.):65-69.

[47] **Kalu** DN. The ovariectomized rat model of postmenopausal bone loss. Bone Miner. 1991;15:175-191.

[48] **Martin** EA, Ritman EL, Turner RT. Time course of epiphyseal growth plate fusion in rat tibiae. Bone 2003;32:261-267.

[49] **Hansson** LI, Menander-Sellmann K, Stenström A, Thorngren KG. Rate of normal longitudinal bone growth in the rat. Calcif.Tissue Res. 1972;10:238-251

[50] **Walker** KV, Kemper NF. Cell kinetics of growth cartilage in the rat tibia.II. Measurements during aging. Cell Tissue Kinet. 1972;5:409-419.

[51] **Sun** H, Qu Z, Guo Y, Zang G, Yang B. In vitro and in vivo effects of rat kidney vascular endothelial cells on osteogenesis of rat bone marrow mesenchymal stem cells growing on polylactide-glycolic acid (PLGA) scaffolds. Biomed. Eng. Online 2007;6:41.

[52] **Hayashi** O, Katsube Y, Hirose M, Ohgushi H, Ito H. Comparison of osteogenic ability of rat mesenchymal stem cells from bone marrow, periosteum and adipose tissue. Calcif.Tissue Int. 2008;82:238-247.

ACKNOWLEDGEMENTS

I would like to thank the AO Research Institute for the opportunity to perform my doctoral thesis at their facility, Prof. Dr. Keita Ito for his supervision and Prof. Pierre Montavon for the academic supervision of this work. A special thank to Dr. Andrea Tami for his great guidance and technical advices and Dr. Stefan Milz and his team from the histology department. Furthermore sincere thank to Christoph Sprecher for his technical aid with the image analysis, Dr. Melanie Pucher for her help in surgery and pQCT and the staff at the AO Institute for supporting me in my work. Last but not least, I would like to thank my family and my friend for their support.

Lebenslauf

Name	Michelle Gertrud Baucke
Geburtsdatum	02.05.1979
Geburtsort	Werneck
Nationalität	deutsch

1985-1989	Primarschule Werneck, Deutschland
1989-1990	Hauptschule Schleerieth, Deutschland
1990-1999	Olympia-Morata-Gymnasium Schweinfurt, Deutschland
06/1999	Abitur
2000-2007	Veterinärmedizinische Fakultät der Universität Leipzig, Deutschland
02/2007	Approbation als Tierärztin an der Veterinärmedizinischen Fakultät der Universität Leipzig
seit 04/2007	Doktorandin am AO Forschungsinstitut Davos und an der Vetsuisse-Fakultät der Universität Zürich (Departement für Kleintiere, Klinik für Kleintierchirurgie), Schweiz

5. Juni 2008